

CLEAN RESOURCES FINAL REPORT PACKAGE

Project proponents are required to submit a Final Report Package, consisting of a Final Public Report and a Final Financial Report. These reports are to be provided under separate cover at the conclusion of projects for review and approval by Alberta Innovates (AI) Clean Resources Division. Proponents will use the two templates that follow to report key results and outcomes achieved during the project and financial details. The information requested in the templates should be considered the minimum necessary to meet AI reporting requirements; proponents are highly encouraged to include other information that may provide additional value, including more detailed appendices. Proponents must work with the AI Project Advisor during preparation of the Final Report Package to ensure submissions are of the highest possible quality and thus reduce the time and effort necessary to address issues that may emerge through the review and approval process.

Final Public Report

The Final Public Report shall outline what the project achieved and provide conclusions and recommendations for further research inquiry or technology development, together with an overview of the performance of the project in terms of process, output, outcomes and impact measures. The report must delineate all project knowledge and/or technology developed and must be in sufficient detail to permit readers to use or adapt the results for research and analysis purposes and to understand how conclusions were arrived at. It is incumbent upon the proponent to ensure that the Final Public Report **is free of any confidential information or intellectual property requiring protection**. The Final Public Report will be released by Alberta Innovates after the confidentiality period has expired as described in the Investment Agreement.

Final Financial Report

The Final Financial Report shall provide complete and accurate accounting of all project expenditures and contributions over the life of the project pertaining to Alberta Innovates, the proponent, and any project partners. The Final Financial Report will not be publicly released.

Alberta Innovates is governed by FOIP. This means Alberta Innovates can be compelled to disclose the information received under this Application, or other information delivered to Alberta Innovates in relation to a Project, when an access request is made by anyone in the general public.

In the event an access request is received by Alberta Innovates, exceptions to disclosure within FOIP may apply. If an exception to disclosure applies, certain information may be withheld from disclosure. Applicants are encouraged to familiarize themselves with FOIP. Information regarding FOIP can be found at <http://www.servicealberta.ca/foip/>. Should you have any questions about the collection of this information, you may contact the Manager, Grants Administration Services at 780-450-5551.

CLEAN RESOURCES FINAL PUBLIC REPORT TEMPLATE

1. PROJECT INFORMATION:

Project Title:	Vanadium Redox Flow Battery (VRFB) – Technology Comparison, Acquisition of Experience, Development of Use Cases and Energy Management Strategies
Alberta Innovates Project Number:	G2019000365 (AI 2514)
Submission Date:	April 27, 2021
Total Project Cost:	\$221,000
Alberta Innovates Funding:	\$98,000
AI Project Advisor:	Paolo Bomben

2. APPLICANT INFORMATION:

Applicant (Organization):	University of Alberta
Address:	85 Ave & 116 St, Edmonton AB T6G 2R3
Applicant Representative Name:	Dr. Petr Musilek
Title:	Professor
Phone Number:	(780) 492-5368
Email:	pmusilek@ualberta.ca

Alberta Innovates and Her Majesty the Queen in right of Alberta make no warranty, express or implied, nor assume any legal liability or responsibility for the accuracy, completeness, or usefulness of any information contained in this publication, nor for any use thereof that infringes on privately owned rights. The views and opinions of the author expressed herein do not reflect those of Alberta Innovates or Her Majesty the Queen in right of Alberta. The directors, officers, employees, agents and consultants of Alberta Innovates and The Government of Alberta are exempted, excluded and absolved from all liability for damage or injury, howsoever caused, to any person in connection with or arising out of the use by that person for any purpose of this publication or its contents.

3. PROJECT PARTNERS

Please provide an acknowledgement statement for project partners, if appropriate.

RESPOND BELOW

A. EXECUTIVE SUMMARY

Provide a high-level description of the project, including the objective, key results, learnings, outcomes and benefits.

RESPOND BELOW

This project examines Vanadium for Redox Flow Batteries (VRFB) and compares them with other electricity storage approaches. The presented survey identifies the main advantages of this technology as long expected lifecycle, low cost, high operational safety and low environmental impact at the end of life. The report describes the process of assembling a VRFB system on an industrial test site and experience gained through its test operation. Operational performance of the battery system has been examined using experiments with the system connected to the mains using a commercial power converter. The project obtained system model, characterized it, and developed and tested a number of battery use cases and strategies. In addition, new inverter topologies were designed that take into account specific properties and characteristics of VRFB systems to improve its power rating and efficiency. The main findings of the project confirmed the suitability of VRFB batteries for operation in Alberta conditions. They are well suited for stationary applications in a number of use cases, including smoothing of renewable generation, load shifting and peak shaving.

B. INTRODUCTION

Please provide a narrative introducing the project using the following sub-headings.

- **Sector introduction:** Include a high-level discussion of the sector or area that the project contributes to and provide any relevant background information or context for the project.
- **Knowledge or Technology Gaps:** Explain the knowledge or technology gap that is being addressed along with the context and scope of the technical problem.

RESPOND BELOW

The main driver of this project is the innovation opportunity of VRFB technology that is expected to bring disruptive changes to the electric power industry. One of the main advantages of VRFB technology is that the power and energy ratings are independent, which allows for long discharge times. This is favourable for stationary applications, ranging from home energy storage systems to large-scale power grid services. They have the potential to provide the response times and capacities necessary for smoothing and shifting intermittent energy resources, thus allowing effective integration of renewable energies and contributing to reduction of GHG emissions from carbon-based energy production.

Although VRFB technology is currently in the stage of demonstration and early commercialization, there are major knowledge gaps related to their use cases, energy management strategies and performance in operational environment. The three main questions to be answered within the project are (i) What are possible uses of VRFB system across the power industry and prosumers; (ii) What types of energy management strategies can be used for various applications and how they can be supported by VRFB-specific power electronics; and (iii) What are the key performance indicators of VRFB systems, how they evolve over time, and how are they affected by electrolyte composition.

C. PROJECT DESCRIPTION

Please provide a narrative describing the project using the following sub-headings.

- **Knowledge or Technology Description:** Include a discussion of the project objectives.
- **Updates to Project Objectives:** Describe any changes that have occurred compared to the original objectives of the project.
- **Performance Metrics:** Discuss the project specific metrics that will be used to measure the success of the project.

RESPOND BELOW

This project addresses knowledge gaps associated with Vanadium for Redox Flow Cells as electric storage devices in comparison with other electricity storage approaches. In particular, we will conduct a detailed, comprehensive survey of energy storage solutions and compare them to Vanadium Redox Flow Battery (VRFB) from a variety of perspectives (steady state and transient efficiencies, fixed and variable costs, lifetime, scalability, safety, environmental impact, parasitic losses, etc.). In addition, with our industrial partners, we will conduct a pilot-scale deployment of actual VRFB battery system to evaluate their performance under different deployment scenarios performing economic and environmental assessment of VRFB technology.

This project has four main objectives:

- To compare VRFB technology with other electricity storage approaches;
- To acquire development and operating experience with VRFB system;
- To design a VRFB-specific voltage convertor to improve system efficiency;

- To develop use cases and energy management strategies for VRFBs.

General strategic metrics we will track:

- Survey of VRFB technology & comparison to other ESS approaches submitted for publication.
- VRFB system installed on site, operational, and collecting data.
- Project experience disseminated to partners and other interested parties (through research report, workshops, and publications).

Technical metrics we will track are:

- Operational efficiency of developed VRFB controller improved in comparison to current, state-of-the-art controllers.
- Developed VRFB use cases expand currently considered standard applications (i.e. beyond utility scale energy storage system).
- Developed operational strategies improve operational efficiency of energy systems in one or several ways (economy, environmental performance, usage of renewable energy, energy availability in isolated systems, provision of ancillary services, etc.).

D. METHODOLOGY

Please provide a narrative describing the methodology and facilities that were used to execute and complete the project. Use subheadings as appropriate.

RESPOND BELOW

Please see attached, detailed report

E. PROJECT RESULTS

Please provide a narrative describing the key results using the project's milestones as sub-headings.

- Describe the importance of the key results.
- Include a discussion of the project specific metrics and variances between expected and actual performance.

RESPOND BELOW

Please see attached, detailed report

F. KEY LEARNINGS

Please provide a narrative that discusses the key learnings from the project.

- Describe the project learnings and importance of those learnings within the project scope. Use milestones as headings, if appropriate.
- Discuss the broader impacts of the learnings to the industry and beyond; this may include changes to regulations, policies, and approval and permitting processes

RESPOND BELOW

Please see attached, detailed report

G. OUTCOMES AND IMPACTS

Please provide a narrative outlining the project's outcomes. Please use sub-headings as appropriate.

- **Project Outcomes and Impacts:** Describe how the outcomes of the project have impacted the technology or knowledge gap identified.
- **Clean Energy Metrics:** Describe how the project outcomes impact the Clean Energy Metrics as described in the *Work Plan, Budget and Metrics* workbook. Discuss any changes or updates to these metrics and the driving forces behind the change. Include any mitigation strategies that might be needed if the changes result in negative impacts.
- **Program Specific Metrics:** Describe how the project outcomes impact the Program Metrics as described in the *Work Plan, Budget and Metrics* workbook. Discuss any changes or updates to these metrics and the driving forces behind the change. Include any mitigation strategies that might be needed if the changes result in negative impacts.
- **Project Outputs:** List of all obtained patents, published books, journal articles, conference presentations, student theses, etc., based on work conducted during the project. As appropriate, include attachments.

RESPOND BELOW

Metrics were defined in the agreement and are listed below along with their current status

General strategic metrics

- Survey of VRFB technology & comparison to other ESS approaches submitted for publication. (COMPLETED)

- VRFB system installed on site, operational, and collecting data. (COMPLETED)
- Project experience disseminated to partners and other interested parties (through research report, workshops, and publications). (IN PROGRESS – will be completed after the final report is finalized)

Technical metrics

- Operational efficiency of developed VRFB controller improved in comparison to current, state-of-the-art controllers. (COMPLETED)
- Developed VRFB use cases expand currently considered standard applications (i.e. beyond utility scale energy storage system). (COMPLETED)
- Developed operational strategies improve operational efficiency of energy systems in one or several ways (economy, environmental performance, usage of renewable energy, energy availability in isolated systems, provision of ancillary services, etc.). (COMPLETED)

Additionally the following general metrics were achieved:

Metric	Value
# of students trained	6
# of publications	3
# of new products / services	0
# field pilots	1

H. BENEFITS

Please provide a narrative outline the project's benefits. Please use the subheadings of Economic, Environmental, Social and Building Innovation Capacity.

- **Economic:** Describe the project's economic benefits such as job creation, sales, improved efficiencies, development of new commercial opportunities or economic sectors, attraction of new investment, and increased exports.
- **Environmental:** Describe the project's contribution to reducing GHG emissions (direct or indirect) and improving environmental systems (atmospheric, terrestrial, aquatic, biotic, etc.) compared to the industry benchmark. Discuss benefits, impacts and/or trade-offs.
- **Social:** Describe the project's social benefits such as augmentation of recreational value, safeguarded investments, strengthened stakeholder involvement, and entrepreneurship opportunities of value for the province.
- **Building Innovation Capacity:** Describe the project's contribution to the training of highly qualified and skilled personnel (HQSP) in Alberta, their retention, and the attraction of HQSP from outside the province. Discuss the research infrastructure used or developed to complete the project.

RESPOND BELOW

Bloomberg New Energy Finance forecasts that the global energy storage market will “double six times” between now and 2030 (to more than 300GWh). An estimated US\$103 billion will be invested in [all types of] energy storage over that time period globally. Technavio forecast, estimates the global VRFB market to grow to US\$140 million by 2021, at a compound annual growth of 9%.

Adoption of VRFB systems by Alberta utilities and residents would bring a significant contribution to renewable energy goals by allowing large incremental number of new solar and wind generation. Longer-term potential could be upwards a few GW by 2030. In terms of employment, using a conservative assumption of 10 Full-Time Equivalent (FTE) employment years per MW installed, 2,000 MW of rooftop solar could sustain on the order of 500 full time jobs per year until 2050.

I. RECOMMENDATIONS AND NEXT STEPS

Please provide a narrative outlining the next steps and recommendations for further development of the technology developed or knowledge generated from this project. If appropriate, include a description of potential follow-up projects. Please consider the following in the narrative:

- Describe the long-term plan for commercialization of the technology developed or implementation of the knowledge generated.
- Based on the project learnings, describe the related actions to be undertaken over the next two years to continue advancing the innovation.
- Describe the potential partnerships being developed to advance the development and learnings from this project.

RESPOND BELOW

As of March 24, 2021, all milestones corresponding to this project goals have been completed. In addition to the originally planned tasks, a novel state-of-charge sensor has been developed. This project addressed knowledge gaps associated with Vanadium for Redox Flow Cells as electric storage devices in comparison with other electricity storage approaches.

At the end of the project, the battery system was moved to the University of Alberta. In the near future, we will continue its characterization and testing. We expect to develop new partnerships with SME partners to explore options for commercial development and use of VRFB systems. Possible partners include Growing Greener Innovations and Nutana Power.

J. KNOWLEDGE DISSEMINATION

Please provide a narrative outlining how the knowledge gained from the project was or will be disseminated and the impact it may have on the industry.

RESPOND BELOW

Progress and results of this project have been presented to the public and professional communities in the province at a number of occasions:

SPARK 2019: Under the title “Flexible batteries to power the renewable transition” and as part of the Future Energy Systems at the University of Alberta, the Vanadium redox flow battery (VRFB) project participated in the SPARK conference hosted in Edmonton at the end of October 2019. The conference, organized by the Emissions Reduction Alberta (ERA), featured a number of energy transition topics and clean technology innovation in general. VRFB showcase pursued to inform the audience about the

technical features and potential environment benefits of the technology toward decarbonizing the power sector.

Telus WoS: In Summer 2019, the VRFB project showcased at the TELUS World of Science Edmonton that hosted a short course called Research Zone in partnership with the UAlberta Energy Week. During the Research Zone training eighteen graduate students and post-doctoral fellows acquire skills that let them to communicate with public audiences, mainly children and youth. The presentation of the VRFB project to kids provided full explanations about how their homes are electrified and the possibilities to store electricity for future use.

APIC: Members of Alberta Power Industry Consortium (APIC) are the major electric power utilities in the province. They include Alberta Electric System Operator (AESO), AltaLink, ATCO Electric, Enmax, EPCOR, and FortisAlberta. Information on this project has been provided to the member companies at a number of venues through the project duration.

K. CONCLUSIONS

Please provide a narrative outlining the project conclusions.

- Ensure this summarizes the project objective, key components, results, learnings, outcomes, benefits and next steps.

RESPOND BELOW

This project was designed to address knowledge gaps associated with Vanadium for Redox Flow Batteries (VRFB) as electric storage devices in comparison with other electricity storage approaches.

The conducted survey of found that VRFB brings a number of advantages, especially in stationary applications with long expected lifecycle. In addition to cycling and cost considerations, VRFB technology also excels in terms of safety and environmental impact at the end of its life. In addition to the study of research literature, a technology and market survey was also executed to complement the review.

The VRFB system has been assembled on an industrial test site and operated to gain experience and to conduct experiments aimed to characterize the installed system and to develop and test use cases and strategies. A number of experiments have been performed to examine performance of the battery system during charging and discharging. The system was connected to the mains using a commercial power converter acquired for the project. In addition, research was conducted to design new inverter topologies that take into account specific properties and characteristics of VRFB systems to increase its power rating, and to improve efficiency and improve cell balancing. In parallel with the experiments, simulation models of the VRFB system have been developed for design and modelling of use cases and operation strategies of the system.

In addition to the activities directly addressing project objectives, additional tasks have been included to deal with issues encountered during project execution. The first was design of an alternative current sensor necessitated by damage to the original control board. The second was development of a state-of-

charge sensor that would be necessary for an effective integration of VRFB system in many different applications.

The results of the project were disseminated through a number of stakeholder communities, including research literature, electric utilities, and general public.

Vanadium Redox Flow Battery (VRFB)

technology comparison, acquisition of experience, development
of use cases and energy management strategies

Final Report to Alberta Innovates

Petr Musilek, Carolina Quiroz-Juarez, Peter Atrazhev, Calvin Schofield,
Nazli Kazemi, Ryan Li, Yuzhuo Li

University of Alberta

March 2021

This document reports on the outcomes of the VRFB project funded by Alberta Innovates under the Bitumen Beyond Combustion program, by the Future Energy Systems research initiative at the University of Alberta, and by ATCO Electricity.

Table of Contents

1. Survey of VRFB Technology	3
1.1 Collection of research/trade literature	3
1.2 A research survey and technology report.....	4
2. VRFB system installation and operation.....	7
2.1 Component acquisition and shipping	7
2.2 System assembly and installation	7
2.3. Installation and configuration of data collection and communication systems	9
2.4 Main data collection period	11
3. VRFB specific power electronics.....	19
3.1 High ratio voltage converter system design	19
3.3 Design of system controller considering cell voltage variation.....	25
4. Use cases and Energy Management (EM).....	27
4.1 Simulation tools	27
4.2 Development of use cases and operation strategies.....	31
4.4 Stakeholder engagement, dissemination	40
5. Additional Topics.....	41
5.1. SOC Sensing - Motivation & Techniques	41
5.2: SOC (Light) Sensor	42
5.3. Microwave SOC Sensor	44
5.4: Alternative Current sensor	47
6. Conclusions	48
7. References	49

1. Survey of VRFB Technology

1.1 Collection of research/trade literature

The interest in energy storage technologies can be tracked centuries back. However, it has recently been reflected by the large market share of battery energy storage system technologies driven by the needs of renewable energy technologies established in the electricity industry.

Particularly for stationary applications, Lead-acid (PbA) and Sodium-Sulfur (NaS) have been two largely employed technologies for decades considering their good technical performance characteristics and relatively low costs. Nonetheless, they have inherent operational safety risks and present environmental concerns. Lithium-ion (Li-ion) technology has been a better option in terms of technical performance; however, it has also safety risks being the technology cost the main obstacle. Under these considerations, the “Vanadium redox flow batteries: a review of use cases for microgrids and comparison with other technologies” survey (the survey) is a comparison of the first three electrochemical battery technologies to Vanadium redox flow (VRF) battery for stationary applications, particularly their use in microgrids.

Electrochemical batteries are essential components of microgrids: 1) can be connected where they are required contributing to the microgrid stability and reliability, 2) can be sized depending on the application power/energy requirements, and 3) contribute to the microgrid’s energy balancing and microgrid islanded operation.

Regarding the emphasis on microgrids, it has been a significant shift in the power system expansion paradigm toward the development of smaller power grids. This is driven by the environmental and technical benefits microgrids represent for system operators and final users, and the existence of technology innovations involving electrical and information infrastructure.

Moreover, the feasible integration of batteries in microgrids heavily depends on the effective identification of application requirements and on the battery technical performance, environmental impact and costs. In this case, it was crucial to identify applications whose requirements can be full-filled by the battery technologies analyzed.

With the literature collection comprising 164 references, the selection aims at giving a broad perspective about the state-of-the-art of the VRFB technology including research in terms of technology innovations and feasible applications, industry status, and government efforts to implement demonstration projects.

Type of reference	No. of references	Approach
Journal / conference	115	Technology research, operation, costs analysis and environmental impact
Book	7	Technology fundamentals and applications

Technology report	17	Technology costs, market potential, applications in the industry, case studies
Project report	8	Government programs in the USA, projects implemented
Industry	15	VRFB manufacturers and projects implemented
Database	1	Department of Energy, Global Energy Storage Database
PhD Thesis	1	Practical application of a VRFB system

Table 1.1.1 References for the VRFB survey

1.2 A research survey and technology report

This project produced a research survey article that overviews VRFB technology, provides a brief historical review, captures the current industry status through 67 identified projects and the most common applications, and tracks previous technology research work. From the industry outlook it can be noticed that most of the VRFB projects have been implemented during the last decade. The main application has been the integration of renewables, and the capacity has been typically between 120 kWh and a few MWh.

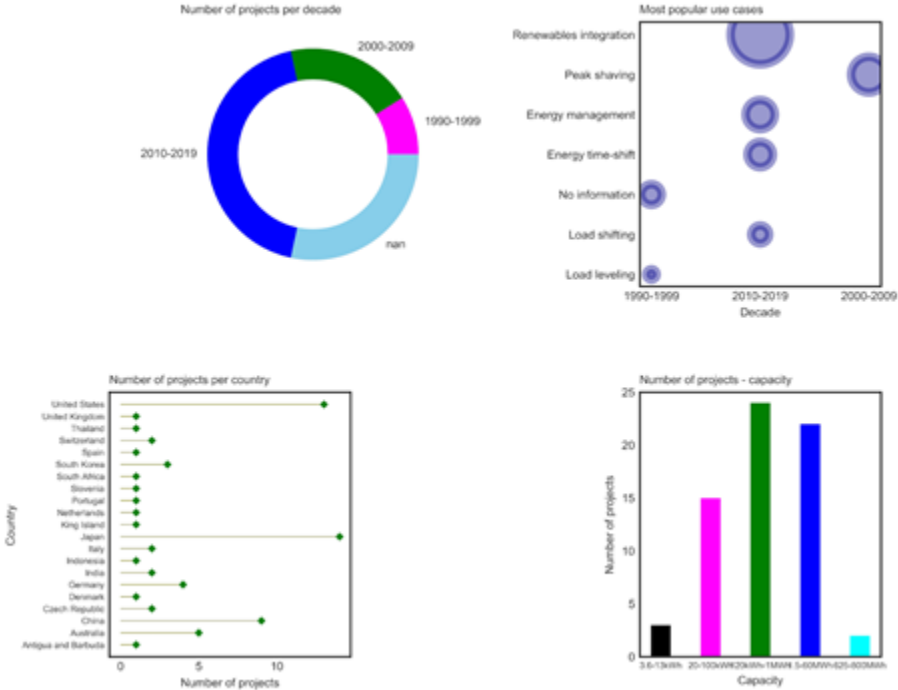


Fig. 1.2.1 VRFB technology overview

Japan was the main equipment provider for the projects analyzed through the company Sumitomo Electric Industries (SEI).

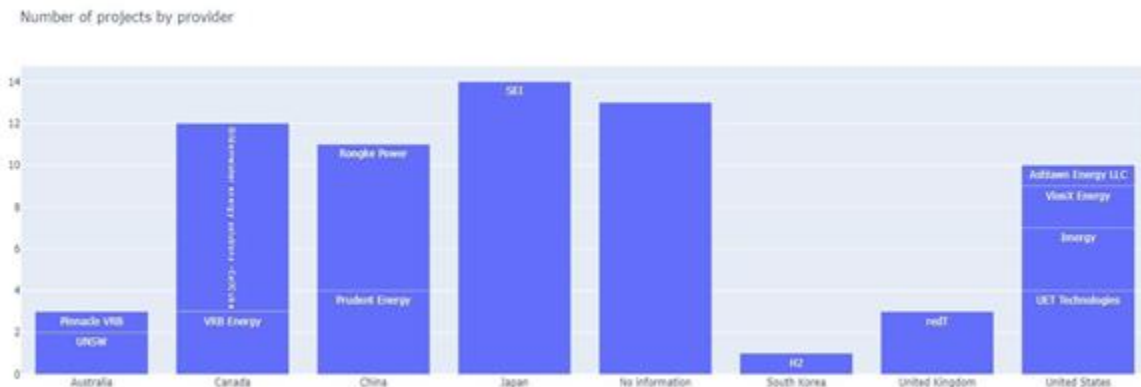


Fig. 1.2.2 Number of projects by provider

During the literature review, there were some contradictions and inconsistencies found, for instance in terms of VRFB system definition of its applications. Considering the importance of such definitions to understand if a battery may solve specific energy needs, the survey lists battery applications and their technical requirements, and also metrics that have been used to evaluate battery costs.

Part four of the survey comprises a brief description of each technology, technical performance characteristics, the applications they have been used for, and specific safety and environmental risks each technology represents for the final user.

Part five highlights the differences of battery technologies. In general, PbA and Li-ion batteries are suitable for short to medium discharge duration applications requiring high power densities, (for instance, in power quality, integration of renewables and voltage support applications). Backup power may be not suitable for both technologies as it requires deep discharge capability. NaS and VRFB are considered long discharge technologies suitable for applications requiring reasonable energy density, long cycle life and deep discharge capability (such as load leveling, load shifting and integration of renewables). Particularly VRFBs for load leveling should be further analyzed because this application requires high battery efficiency.

In terms of costs, the analysis is highly dependent on the battery strategy operation. However, when comparing capital costs, PbA is the lowest cost option, followed by VRFB and NaS, with Li-ion being the most expensive option. PbA takes advantage of low investment costs and despite its short cycle life seems to be the best option for small scale stationary applications. If the application is of a larger scale and requires more intensive use, PbA advantages vanish and NaS is the most suitable technology. Furthermore, if the cycle frequency also increases, then the VRFB becomes the better option.

Life cycle assessment methodology has been used by some authors (reference 136 in the survey) to assess the potential environmental impact of battery technologies. According to the authors,

for stationary applications, the battery usage is the main contributor to the environmental impacts. This means that higher round-trip efficiency batteries should be considered first. In this sense, Li-ion should be considered first and VRF last. Nonetheless, there is another important factor to be taken into account: safety. And this is where VRF is the technology with lower risks.

The technology report “Market progress of the Vanadium redox flow battery technology: overview of the market development” complements information about former and current companies manufacturing VRF battery systems, Government programs looking forward to the implementation of the technology and dedicated research initiatives and investigation centers. Both documents are attached with this report.

2. VRFB system installation and operation

2.1 Component acquisition and shipping

Suitable VRFB components were selected from around the world, including the United States, United Kingdom and Germany. The following items have been obtained for use in the VRFB system:

1. VRFB Stack
2. Vanadium electrolyte
3. Inverter/charger
4. Pressure sensors, flow meters, data acquisition unit
5. Aluminum frame for VRFB system
6. Electrolyte tanks, startup cylinders and pumps
7. SOC sensor light source, detector, housing
8. Nitrogen cylinder and pressure regulator
9. Tubing, fittings
10. Safety equipment (eye wash station, chemical resistant gloves)

Most of these items were acquired prior to late August 2019. During the ongoing assembly and testing process, small design changes were made based on experimental observations. The main components acquired as a result of this are the components for the state of charge (SOC) monitoring device (item 7), which is able to estimate SOC via the electrolyte color changes during cycling. Other components (especially tubing/fittings) have been continuously ordered based on the design requirements, as with consumable items such as the nitrogen gas and chemical resistant gloves. The total cost of materials for the project was ~\$13000.

2.2 System assembly and installation

The stack is the central component of the battery system and was purchased from Volterion, a German company that specializes in producing flow battery stacks. The stack consists of 40 cells with a nominal power output of 2.5 kW and a maximum operating pressure of 1 bar. Two 83L polyethylene plastic tanks were selected to hold the positive and negative electrolyte solutions. In order to account for the expected pressure drop across the stack, high-power centrifugal pumps with a maximum flow rate of 28.4 LPM and head pressure of 1.73 bar were selected. Rather than connecting the pumps directly to the outlet of the electrolyte tanks, start-up cylinders with capacities of 5.1L were installed as intermediary reservoirs of electrolyte solution between the main electrolyte tanks and pumps. This was done to minimize the possibility of a major leak occurring at the outlet of the main electrolyte tanks. Downstream of each of the two pumps, a flow meter with a flow range of 0.4 - 18.9 L/min was installed inline with the tubing. At the positive and negative inlet and outlet ports of the stack, a pressure sensor with a maximum range of 1 bar was installed to track the inlet flow pressure and ensure it remained at less than 1 bar as well as to determine the pressure drop across the stack. The positive and negative electrolyte flows were then directed back to their respective electrolyte tanks. To control the flow rate of the pumps and

read the flow meter and pressure sensor measurements, a National Instruments DAQ 6211 unit was acquired and connected to a laptop via USB. A LabVIEW program then enabled pump control and data acquisition. Figure 2.2.1 provides an overview of the piping and instrumentation, while a more general layout of the experimental setup and electrolyte flow path can be seen in Figure 2.2.2.

Figure 2.2.1: A piping and instrumentation diagram (P&ID) of the VRFB system assembly

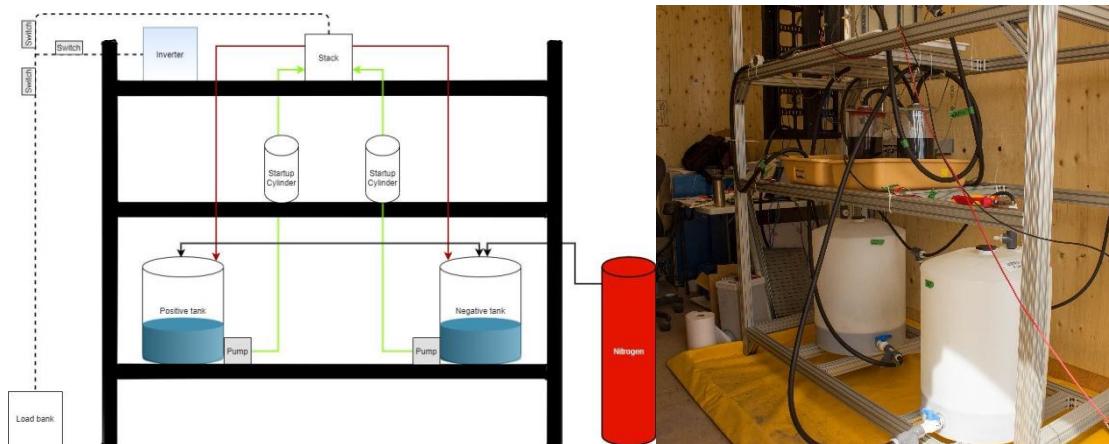
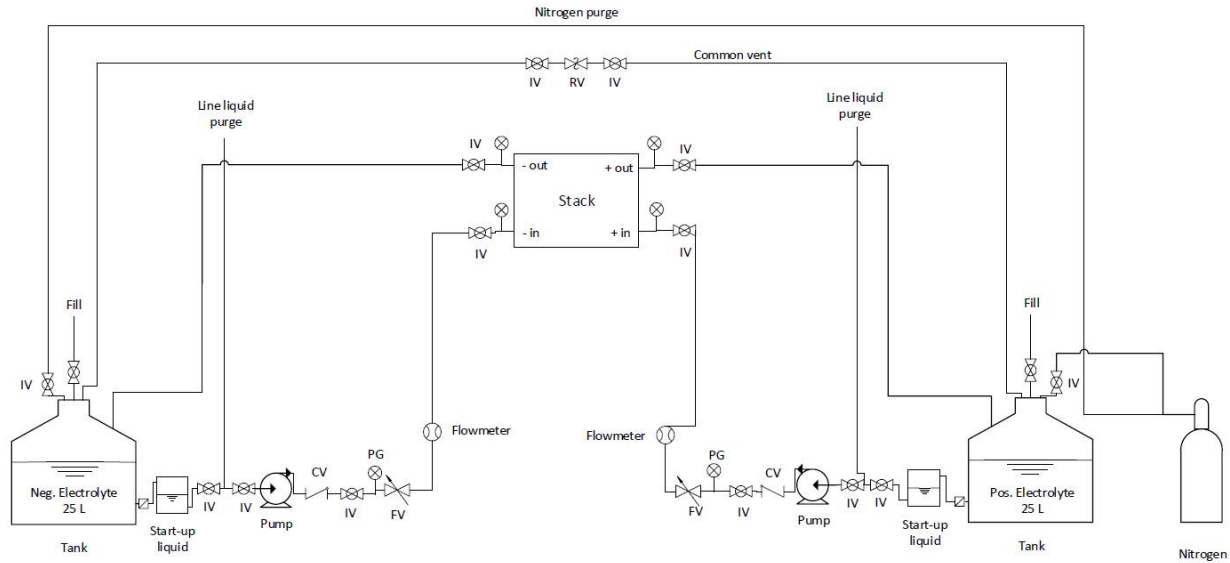


Figure 2.2.2: a) Schematic of the VRFB design and electrolyte flow b) VRFB assembly installed at Nisku site

Once all necessary parts were acquired, the battery and frame were partially assembled at the University of Alberta to perform preliminary tests with deionized water for functionality testing and verification, and to check for leakages. Ease of setup was considered in frame components selection. As such, the setup procedure was relatively simple and could be done with minimal equipment (hex screws, screwdrivers). Initial testing revealed that the startup cylinders

were not built with a stiff enough material and could not handle the forces provided by the pumps. This problem was mitigated by rebuilding the startup cylinders with a stiffer material.

The battery assembly was partially disassembled and moved to the ATCO Nisku site on July 10, 2019 in-coordination with the on-site technicians. After reassembly at the ATCO site, a test run was performed successfully with deionized water in place of electrolytes, and both pumps running simultaneously. A leakage test was performed on August 23, 2019, which confirmed that the system is watertight. Nitrogen pressure tests were conducted afterwards which revealed that the system was not perfectly airtight. While the design does not allow for perfect airtightness (oxygen can diffuse through plastic, ex the electrolyte tanks), improvements were made to limit this including simplification of the tank inlet/outlet connections. The startup cylinders were later identified as one of the main leak sources, and were removed as discussed in section 2.4. Other additions include the auto-rebalancing mechanism (for periodic or automatic remixing of the anolyte/catholyte) discussed in section 2.4, and the SOC sensors (optical and microwave) discussed in Section 5.

2.3. Installation and configuration of data collection and communication systems

The data collection and communication systems were picked to work well with the stack that was selected. The mechanical system data collection measured and recorded flow rate of electrolyte at the ingress and egress points of the stack in order to monitor the health of the stack and detect any flow problems in the stack. Additionally, pressure was measured at the intakes and exhausts of both the negative and positive fluid circuits to monitor for any rise in pressure that may indicate damage in the stack. The mechanical system also recorded the pump speeds for each of the pumps.

The electrical system data collection was initially performed by the Stack Controller purchased from Voltarion. This device was capable of measuring the voltage and current coming from the stack during charging and discharging. Voltages were measured on 3 independent voltmeter inputs and were averaged to get more stable readings.

The main additions to the data collection and communication systems were in the realm of data storage. The system diagram has expanded to include the two new subsystems described in the following text and shown in Figure 2.3.1.

2.3.1: Unified database for data storage: After the data collection systems were configured and the initial tests were performed, a unification of data collection was implemented. The data which was initially stored in csv files was now stored in a local SQLite database. Csv files were kept as redundant data stores. This upgrade allowed for easier and more programmatic data comparison.

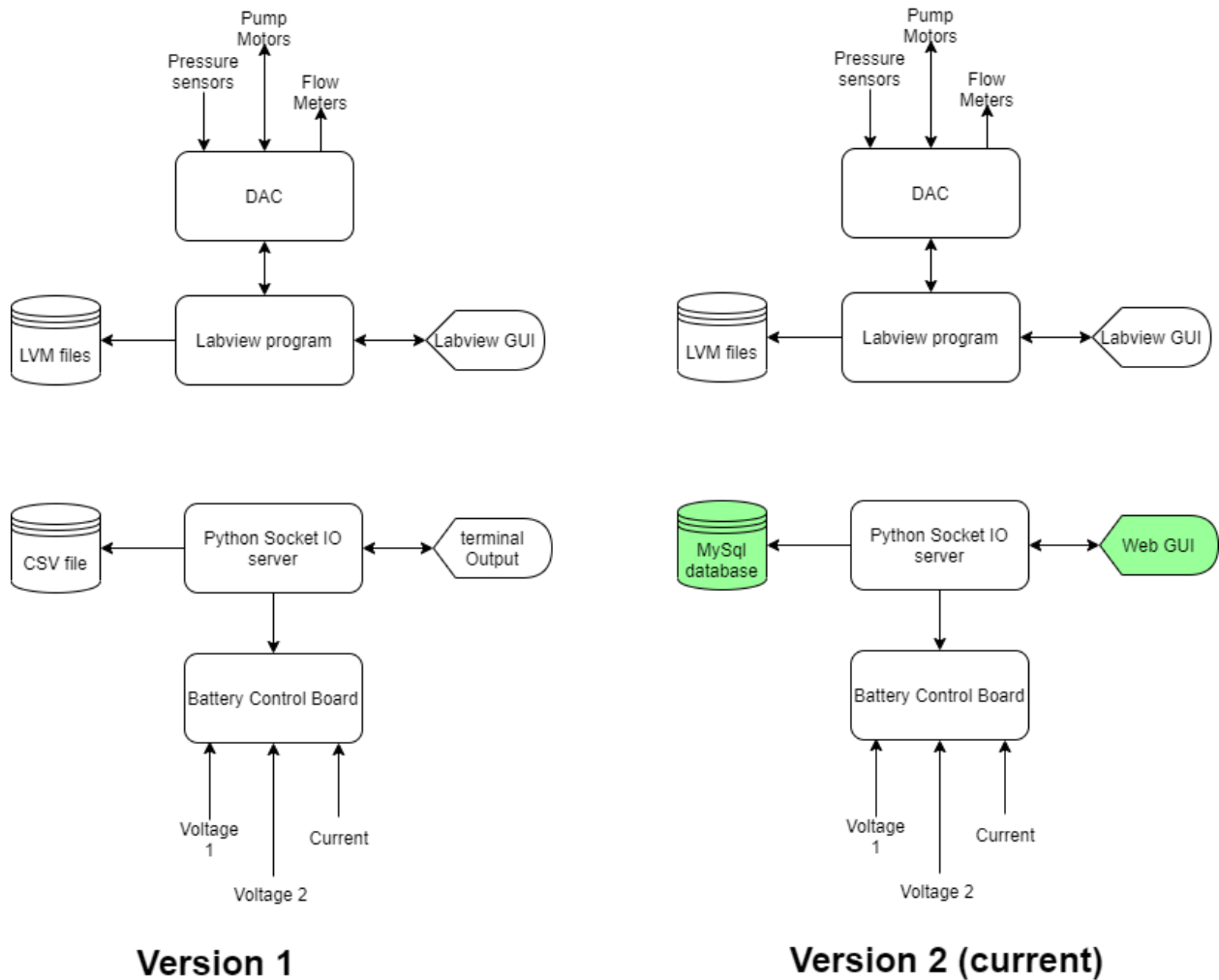


Fig. 2.3.1. Comparison of Version 1 architecture and version 2 architecture

2.3.2: Graphical User Interface: A web based graphical user interface was developed to be used to monitor the voltage and the current from the stack. This was being extended to have the values from the Pressure sensors and the Flow meters. This system would be used to monitor all battery processes from one unified application.

2.3.3: Technical challenges: During the main data collection period, the Voltarion stack controller was damaged and rendered inoperable. The solution that was used is described in section 5.3.

2.4 Main data collection period

2.4.1 Startup Cylinders (~8 L of electrolyte)

Manual Rebalancing Method: Testing was first performed on the startup cylinders utilizing ~8 L of electrolyte. Charging was performed with the Quattro with a max current of 10 A until reaching 58 V. The charge process consists of 2 utilized stages, a constant-current “Bulk” mode at low SOC, and a constant-voltage “Absorption” mode at high SOC. The charge process was considered complete at 0.5-1 A, before the inverter is allowed to enter the 3rd (unutilized) trickle charge “Float” mode. As seen in Figure 2.4.1a, the current is unable to ramp up to the maximum (10A) during the absorption mode, especially during repeated cycling. The cumulative energy input in Figure 2.4.1b shows that the first cycle consumed double the amount of energy as the following cycles. This is due to self-discharge prior to the test, resulting in a chemistry below 0% SOC (ex $V^{3.5+}$ in both tanks) which must be ‘pre-charged’ to V^{3+}/V^{4+} before regular cycling to V^{2+}/V^{5+} .

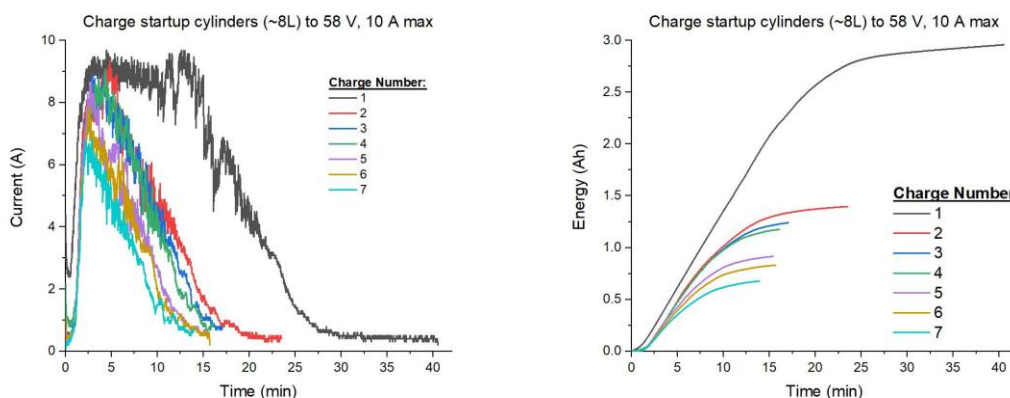


Figure 2.4.1: May 29 charge cycle a) currents and b) Ah energy input

Discharging was done through a three-phase resistor box with maximum currents reaching 5-5.5 A. As predicted from the Nernst equation, the voltage plateaued until reaching 40-45 V and rapidly decreasing (Figure 2.4.2a). As expected, the energy output of the first cycle was not very large with respect to future cycles as with the charge process. During regular cycling, the system is discharged until the OCV drops below 40 V, corresponding to the V^{3+}/V^{4+} redox couple. As such the first cycle had a reduced efficiency of ~40%, while the remainder of the cycles had efficiencies of 60-85%.

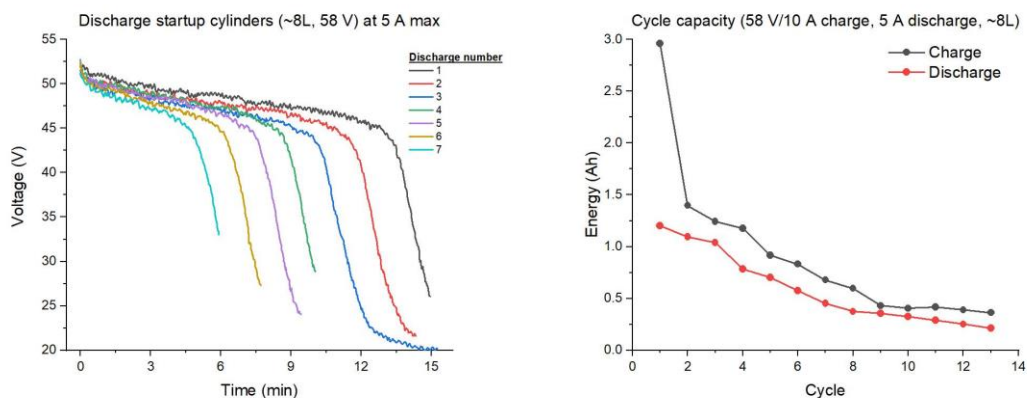


Figure 2.4.2: Startup cylinder a) discharge curves (May 29) b) charge/discharge capacities (May 29, June 5)

However, both the discharging time and capacity were observed to decrease by nearly $\frac{2}{3}$ over the course of seven cycles (Figure 2.4.2b). The cycling process was accompanied by an observable volume shift from the positive to the negative chamber. This behavior can be expected due to preferential ion and water transfer across the anionic membrane [10], or due to flowrate mismatches between the positive/negative half-cells. Although reducing these mismatches resulting in smaller and more predictable capacity losses (cycles 8-13), it was not eliminated entirely.

As this is a symmetrical degradation mechanism, manual rebalancing (i.e. periodic remixing of the electrolytes) can be done to recover some of these capacity losses. Full recovery is generally not possible with this method due to asymmetrical mechanisms such as hydrogen evolution, $V(V)$ precipitation, or $V(II)$ oxidation with atmospheric oxygen. Chemical or electrochemical regeneration techniques are required to recover capacity losses from these mechanisms.

Automatic Rebalancing Method: In order to mitigate the previously seen volume change issues, an automatic-rebalancing mechanism was installed between the two tanks. The tanks are connected via a tube with a controllable on/off valve, which (when open) acts as a hydraulic shunt which keeps the electrolyte levels constant.

This concept showed promising results in other studies [10] and was tested in Figure 2.4.3. Cycles 1-4 were performed with a max current of 10 A, which was decreased to 5 A in cycles 5 and 6. (interchange between these charge currents is marked green). This did not significantly change the electrolyte's storage capacity, but the efficiency was slightly increased. Prior to cycle 6, the auto-rebalancing on/off valve was opened, allowing for volume balancing. This was shown to recover some of the lost capacity, as marked in blue in Figure 2.4.3.

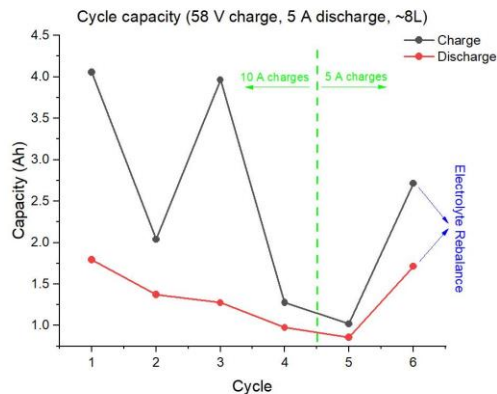


Figure 2.4.3: June 11/12 startup cylinder (~8L) capacity data. All cycles were charged until 58 V and discharged at 5 A. Cycles 1-4 were charged at 10 A max, cycles 5-6 were charged at 5 A max. Cycle 6 proceeded with the automatic rebalancing tube mechanism

2.4.2 Large Tanks (~40 L of electrolyte)

Initial Low-Current Tests: It was later found that the volume change problem was primarily being caused by a startup cylinder pressure leak. After repeated attempts to seal it, it was still unable to hold a pressure. As such, the big tanks (~40 L), were wired to the stack directly without the startups. The auto-rebalancing mechanism is once again used to keep electrolyte volumes constant. A schematic of this design change is shown in Figure 2.4.4. When automatic-rebalancing was used in the previous section, it was located between the startup cylinders, as opposed to between the big tanks in the current design.

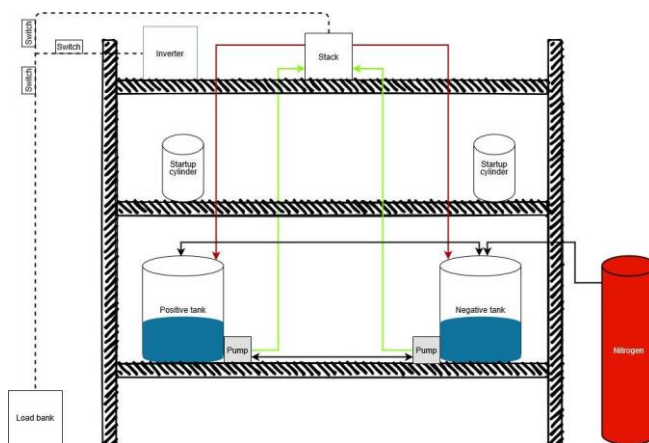


Figure 2.4.4: Schematic of the VRFB design and electrolyte flow without startup cylinders, and utilizing the automatic electrolyte rebalancing method

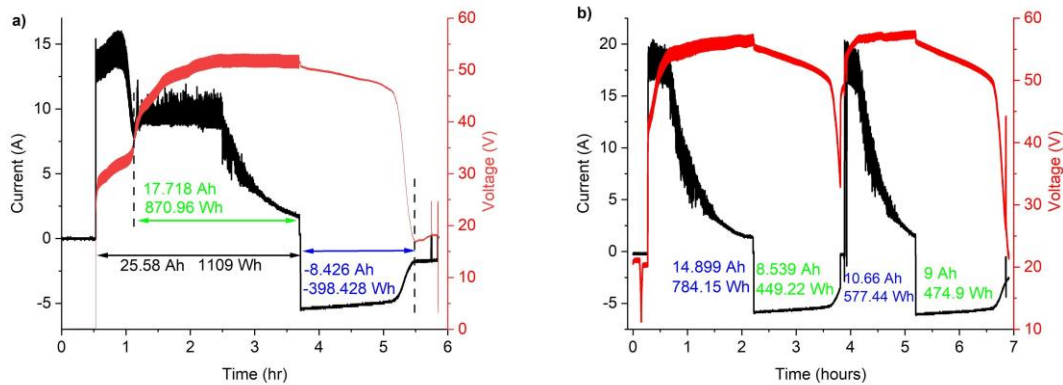


Figure 2.4.5: Charge/discharge curves from a) June 18, b) June 19

A capacity of ~800 Wh is expected (20 Wh/L), which was observed during charging. Smaller values were observed for the discharge process, possibly due to lower current being applied (higher overpotentials during the charging process). Another contributing factor may be ion transfer across the auto-rebalancing mechanism during charge/discharge. Although directional (volumetric) flow primarily occurs due to volume differences, it can behave similar to a salt bridge when static (essentially introducing an extra self-discharge source). An increase in ion transfer rate may increase the required Ah during charge, and decrease the Ah obtained during discharge. Partially closing the rebalancing tube (or using a smaller tube) may improve this performance. Other options include only opening every x cycles, or using a monitoring system such as tank weight to control when the valve is opened. For storage of the electrolyte, particularly at high SOC, it is recommended that this tube remain closed.

OCV-SOC Curves (With New Voltage Sensor): Voltage reading errors also played a role in affecting charge/discharge data. A new voltage sensor was hooked up which provides more accurate readings (matches more closely to inverter and multimeter readings). This can be observed in Figure 2.4.6, where the battery was fully charged, allowed to relax for 45 minutes, then discharged in 5 minute segments with 10 minute delays between measurements (in order to record open circuit voltage). A single-cell (external to the 40 cell stack) could be constructed to provide real-time OCV measurements and assist in SOC monitoring. However, these can be expensive to construct, and only an estimate is required in this case for the estimation of system parameters.

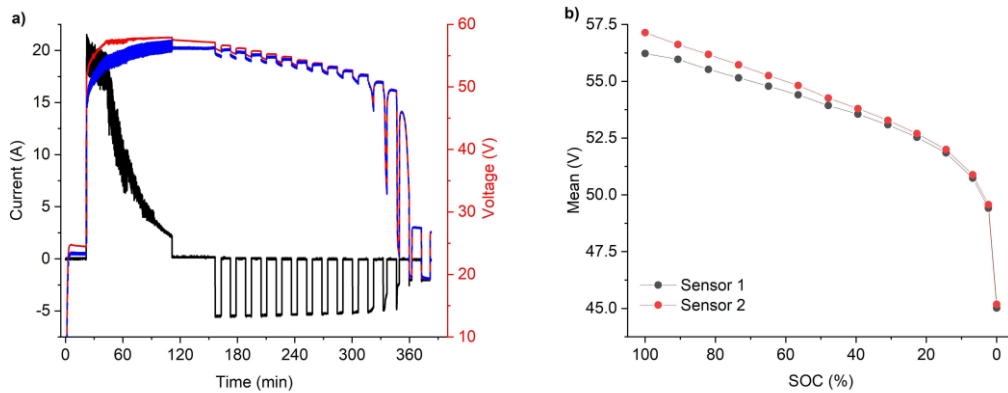


Figure 2.4.6: a) Full I-V data from June 25. Black line = applied current, blue dashed line = original voltage readings, red line = readings from new sensor, b) open-circuit voltage readings

The 45 & 10 minute relaxation periods (after charging and measurements respectively) were initially chosen based on previous experiments investigating Li-ion batteries. This test found that the voltage stabilized much faster, with no benefit after ~5 minutes in almost all cases. More time was required near 0% SOC due to the low ratios of V(II) and V(V). The low time requirements vs Li-ion batteries can be attributed to the lack of solid-state reactions occurring in the cell.

This test was repeated based on these results. A reduction in the delays to 5 min allowed for additional more precise data points to be obtained in the top/bottom SOC ranges (Figure 2.4.7a). This test also allows the relationship between terminal voltage and OCV to be explored (Figure 2.4.7b).

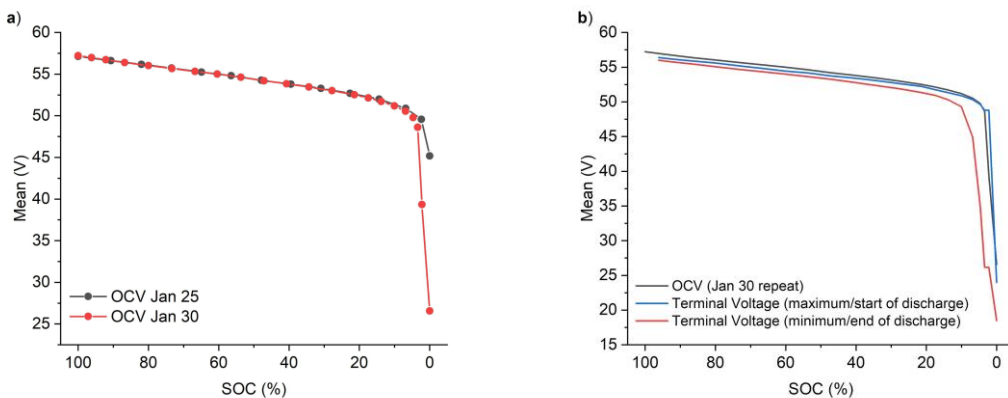


Figure 2.4.7: OCV-SOC test from Jan 30, a) compared to Jan 25, b) compared to terminal voltages

Effect of Charging Current: The effect of charging current was investigated in order to determine its effect on battery performance. Numerous cycles were performed using maximum charging currents of 15 A (Figure 2.4.8) and 30 A (Figure 2.4.9), with a cutoff current of ~1-1.5 A once reaching 62 V. In both cases, discharging was done through a resistive load with a maximum current of 6 A.

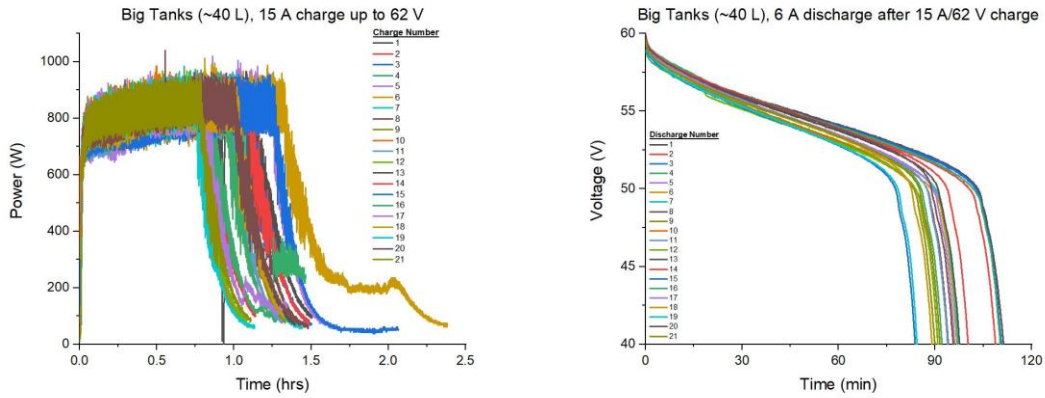


Figure 2.4.8: a) 15 A charge cycles following b) 6 A discharge cycles. All cycles were charged to 62 V and utilized the auto-rebalancing mechanism

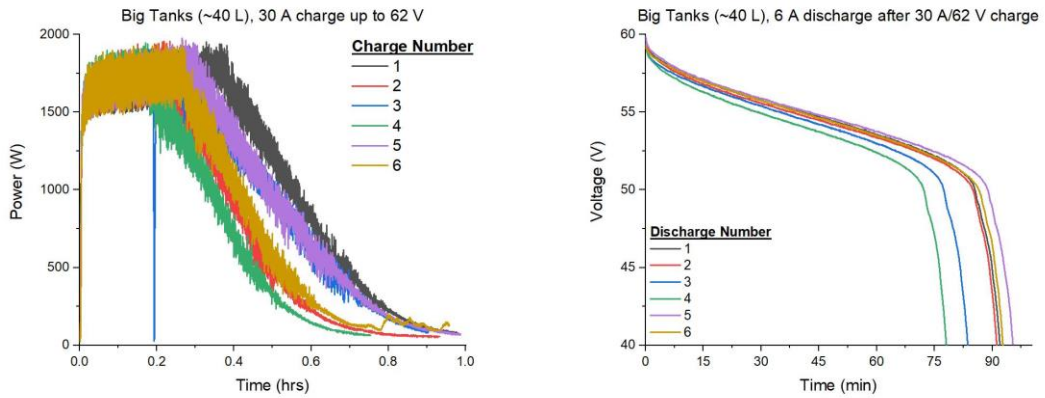


Figure 2.4.9: a) 30 A charge cycles following b) 6 A discharge cycles. All cycles were charged to 62 V and utilized the auto-rebalancing mechanism

Input and output energy was calculated for each cycle (Figure 2.4.10), along with the corresponding cycle efficiencies (Figure 2.4.11). None of these parameters appeared to change significantly as a result of increasing the charge current. With higher currents, although the overpotentials are higher during the bulk of the constant-current charge process, the discharge cycles are primarily responsive to the final cutoff values from the constant voltage regime (62 V/~1-1.5 A). The initial small decrease in output energy can be attributed to variations in the cutoff current.

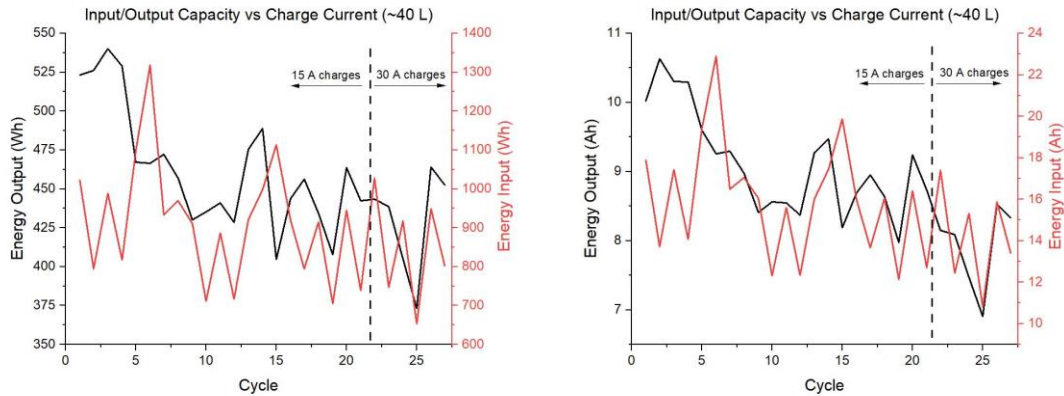


Figure 2.4.10: VRFB input/output capacity during cycling for ~40L of electrolyte: a) Wh capacity, b) Ah capacity. The dashed line separating cycles 21/22 marks a transition between 15 A and 30 A (max) charging current.

Theoretically, input energy could increase with charge current due to the larger amount of losses due to heat production. This could be observed via a decrease in the efficiency, which was not observed in Figure 2.4.11. However, the reduced charging time decreases the self-discharge rate through the automatic rebalancing mechanism, possibly counteracting and masking this effect.

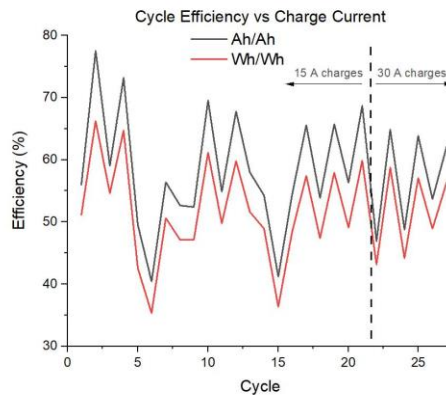


Figure 2.4.11: VRFB efficiency during cycling for ~40L of electrolyte. The dashed line separating cycles 21/22 marks a transition between 15 A and 30 A (max) charging current.

Effect of Discharging Current: The effect of discharging current was also investigated. The maximum charge current was set to 40 A, with cutoff values of 62 V/1-1.5A as in previous experiments. A new resistor set (General Electric IC5891G, catalogue number 5860, 0.6 Ω x 3 resistors) was used to increase the discharge current to a maximum of 47 A. Data from the cycling process can be found in Figure 2.4.12; extracted capacity values are compared to other experiments in Figure 2.4.13.

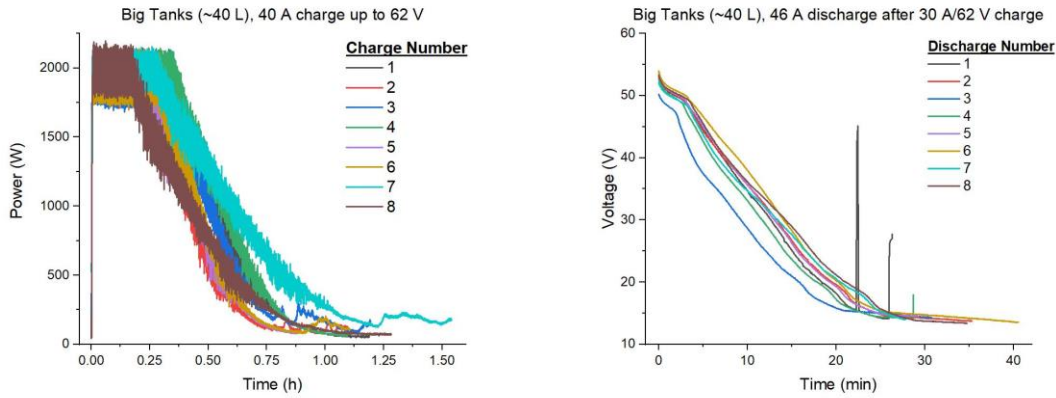


Figure 2.4.12: a) 40 A charge cycles and following b) 46 A discharge

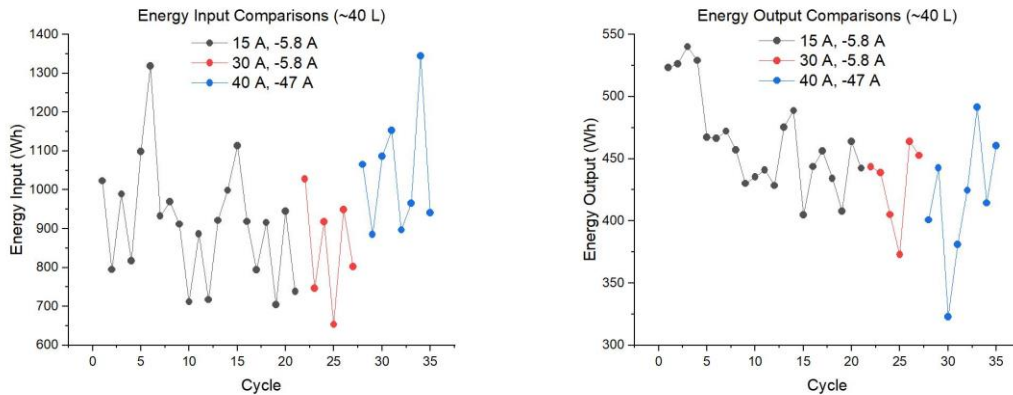


Figure 2.4.13: a) energy input and b) energy output comparisons at different charge/discharge currents

Compared to previous experiments, a small increase in input energy was observed (Figure 2.4.13a), likely due to the higher charge current and overpotentials. Energy output also increased slightly versus previous experiments. However, the voltage data now decreases in a relatively linear fashion until near 0% SOC, no longer following the Nernst equation as expected. Because of this difference between theoretical and experimental results, battery SOC monitoring becomes more difficult.

Due to the high overpotentials, experimental charging currents of ~ 37 A were observed, lower than the set maximum. This is similar to the results obtained when attempting to use 10 A with 8L of electrolyte. Increasing the amount of electrolyte is required to increase the capacity so the inverter may ramp up to the 40 A maximum before switching into the constant voltage regime. The discharge process provides additional support for increasing the amount of electrolyte; it is likely that increasing the amount of electrolyte will improve the capacity such that voltage results are improved at high-current (slower variations in the discharging current and larger area under curve to generate more accurate readings and a larger voltage plateau). Because of these factors, the capacity/power ratio can be considered an important design decision and could be optimized for future applications.

3. VRFB specific power electronics

3.1 High ratio voltage converter system design

3.1.1 Power converter configuration and topology selection for VRFB

As the DC-source/load in the system, VRFB normally has a low voltage (e.g. around 48V). To guarantee a reasonable operation range of the interface converter between VRFB and the utility grid, the AC-DC topology should have a high voltage ratio. Compared to non-isolated solutions, topologies with magnetic isolation are a good choice for the safety and galvanic requirement concerns.

For a low power rating scenario, single-phase isolated converters can be implemented. The commercialized product (MultiPlus-II 48/5000/70-50) has been selected to fulfill the basic charge/discharge operation of the VRFB system. However, with the increase of the power ratings, the overall performance of single-phase configuration will suffer from the bulky DC energy buffers. For an increased power rating scenario, a three-phase isolated configuration is normally adopted to provide a higher power capacity. There are two different structures in practice: (i) single-stage power conversion, (ii) two-stage power conversion.

The two-stage configuration is shown in Fig.3.2.1.1. It consists of two power conversion stages: the first stage is for bi-directional power conversion between AC and DC, the second stage converts the DC power between the high-voltage DC power (stage-1) and the low-voltage DC-power (battery). A typical two-stage power converter is shown in Fig. 2, which uses a conventional 2-level voltage-source converter as stage-1, and a Dual-Active-Bridge (DAB) converter as stage-2.

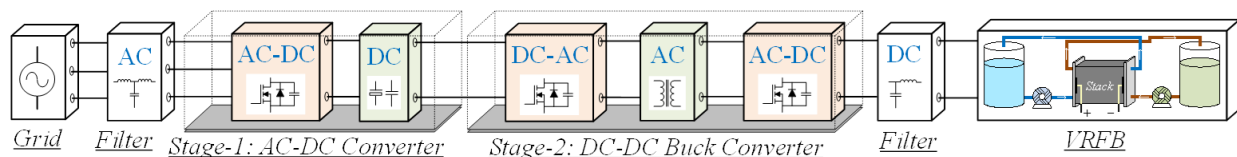


Fig.3.2.1.1. Two-stage power conversion.

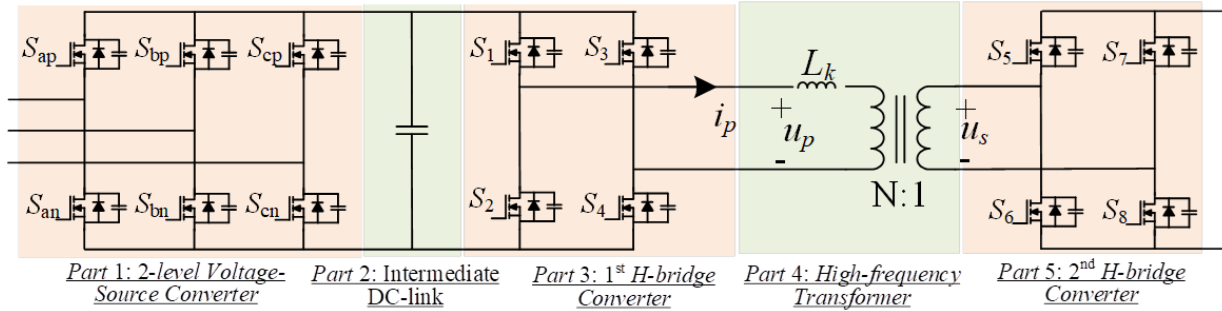


Fig.3.2.1.2. Two-stage power conversion enabled by Dual-Active-Bridge (DAB) converter.

The single-stage configuration is shown in Fig.3.2.1.3. It consists of only one power stage, which can achieve the same function as a two-stage solution, i.e. bi-directional power conversion between AC and DC with voltage buck capability. However, the power conversion loss of a single-stage solution can be inherently less than the two-stage one due to fewer power stages. Therefore, the single-stage configuration is considered in this project as a promising alternative for the VRFB converter system.

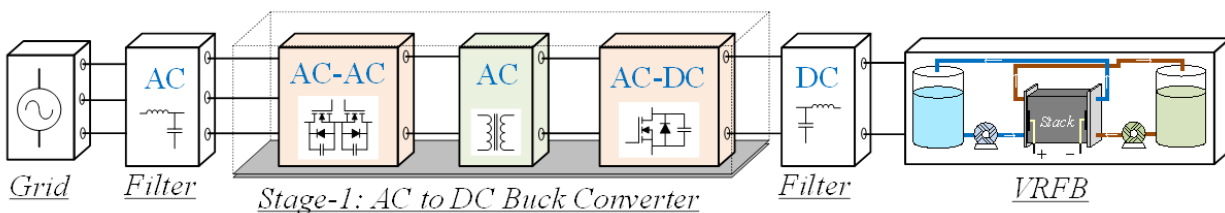


Fig.3.2.1.3. Single-stage power conversion.

In detail, the Isolated Matrix Converter (Iso-MC) is utilized here for the single-stage power conversion. The detailed circuit is shown in Fig.3.2.1.4. Compared to the DAB enabled solution, it enjoys some good features:

1. Single-stage power conversion with potentially lower power processing losses.
2. No intermediate DC-bus devices, which avoids the DC capacitor failures with a lower converter footprint.
3. Soft-switching techniques, which can effectively reduce the switching losses and improve the overall charging/discharging efficiency.
4. Lower dv/dt on the AC-side, which reduces the EMI and avoids unwanted overvoltage problems under a long cable environment.

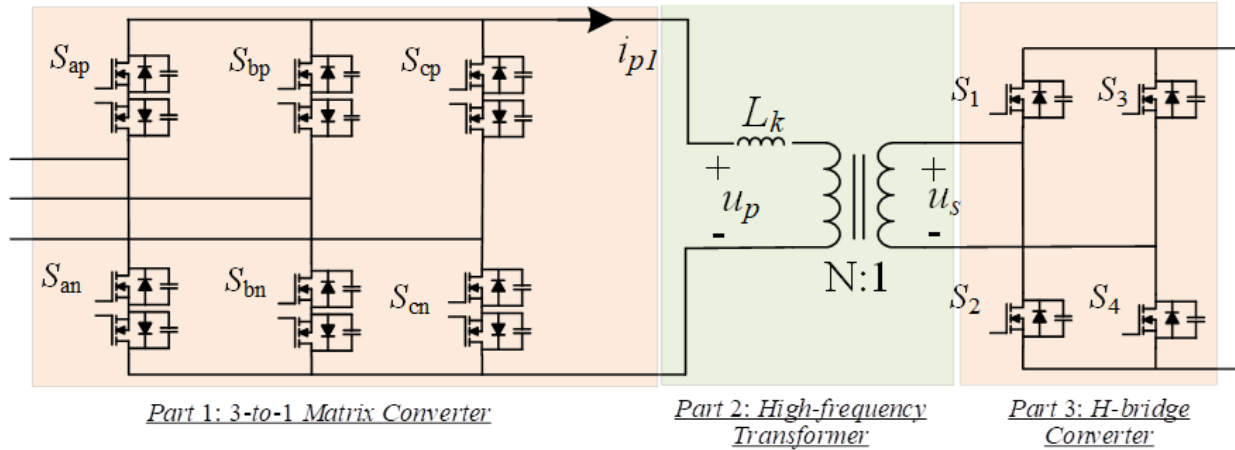


Fig.3.2.1.4. The topology of the isolated matrix converter.

3.2.2 Scalability of the Isolated Matrix Converter for VRFB system

The decoupling of power and capacity is one of the unique advantages of VRFB. To bring down the operation cost of the VRFB, a large enough capacity and power rating could be reasonable to outperform the other competitors. A larger energy capacity can be achieved by simply cascading more tanks of electrolytes (L.F. Arenas, 2017) as shown in Fig.3.2.1.5.

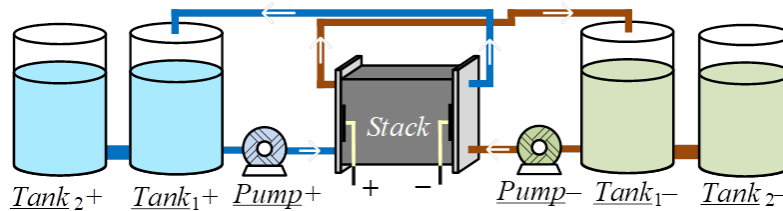


Fig.3.2.1.5. Cascading tanks for increased capacity of VRFB.

On the other hand, there are several ways to increase the power: (i) increase the chemical reaction area for the higher current rating, (ii) using advanced membranes for higher current/voltage ratings, (iii) increase series cell numbers for higher voltage rating, (iv) multi-stack configuration with the limited number of cells in each stack. In practice, a larger reaction area could bring a great challenge for even distribution of current density within the battery. The increased voltage potentials of too many cells integrated into one stack could be too high and lead to higher shunt current. Therefore, for a given membrane material, the 4th way could be a good choice. In detail, the Hydraulic-Parallel-Electrical-Series configuration (L.F. Arenas, 2017) is recommended as shown in Fig.3.2.1.6.

To improve the operation efficiency, low shunt current and low pump loss are desirable, which is highly related to the piping system design (Qiang Ye, 2015). To achieve a low shunt current: (i) the number of cells in a single stack cannot be too high, (ii) branches should be long and thin, (iii) the channels should be wide and long. To get a low pump loss: (i) the branches should be short and thick, (ii) the pumping speed can be controlled as a variable. However, the appropriate pipes

for these two goals are contradictory to each other. To compromise the trade-offs, the multi-stack configuration with thicker and longer branches could be a promising choice. Moreover, to guarantee the compactness of the system, the coil configuration of the piping system should be considered as shown in Fig.3.2.1.7 (Qiang Ye, 2015).

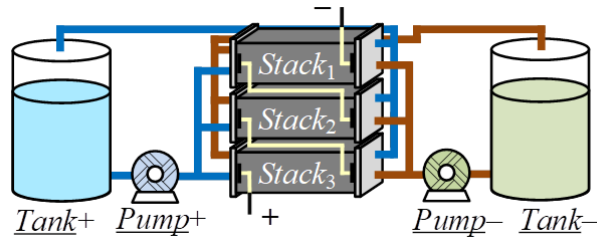


Fig.3.2.1.6. Hydraulic-Parallel-Electrical-Series configuration with multi-stack VRFB for increased power rating.

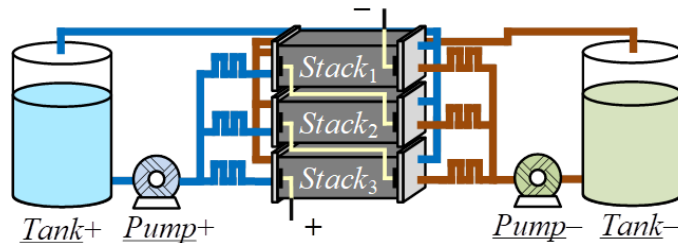


Fig.3.2.1.7. Multi-stack VRFB with coil piping system.

To cope with various VRFB stack configurations, four different structures of power converters can be considered: (a) centralized single converter, (b) AC-parallel-DC-parallel-connected converters, (c) AC-parallel-DC-series-connected converters, (d) AC-parallel-DC-independent-connected converters.

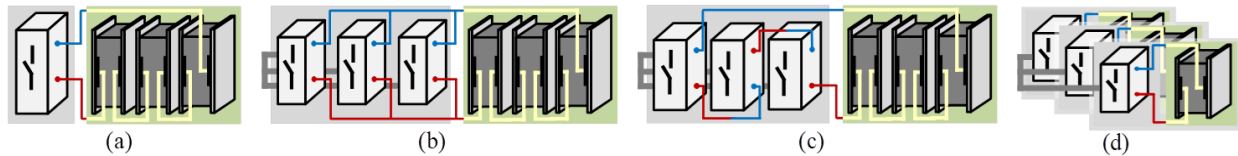
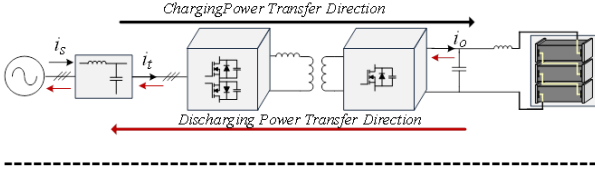
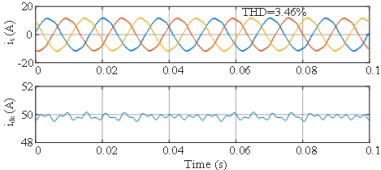
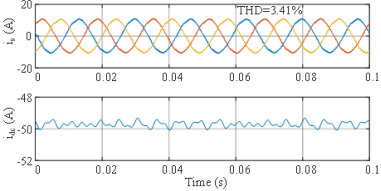
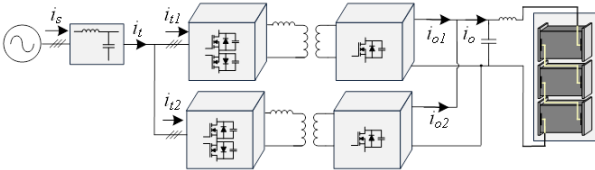
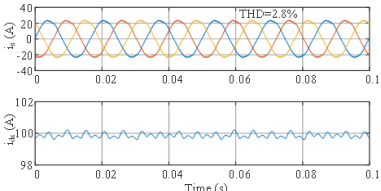
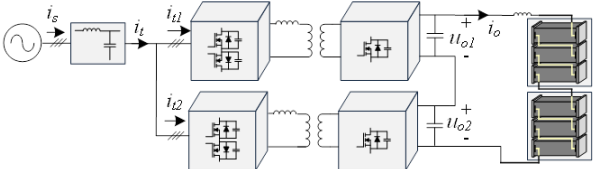
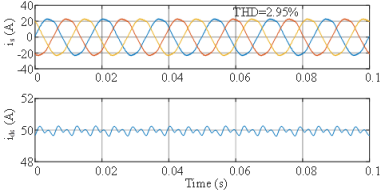
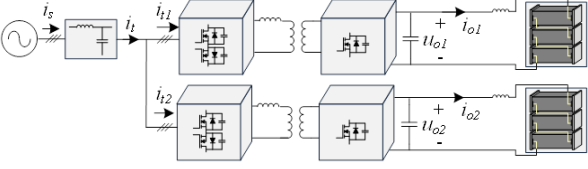
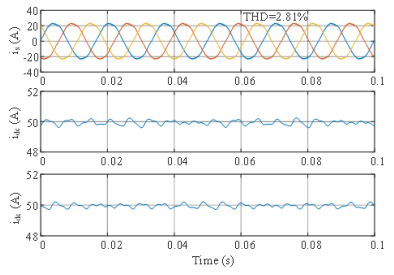


Fig.3.2.1.8. Four different converter structures for multi-stack VRFB. (a) Centralized single converter, (b) AC-parallel-DC-parallel-connected converters, (c) AC-parallel-DC-series-connected converters, (d) AC-parallel-DC-independent-connected converters.

In Table 3.2.1, the operation of all four cases are verified in MATLAB/Simulink. The output Total Harmonic Distortion (THD) can be maintained within a low level and compatible with the Grid Code. In general, the Iso-MC power system shows great flexibility and feasibility for coping with different VRFB stack configuration.

Table 3.2.1. Summaries of four different Iso-MC configurations for Multi-Stack VRFB.

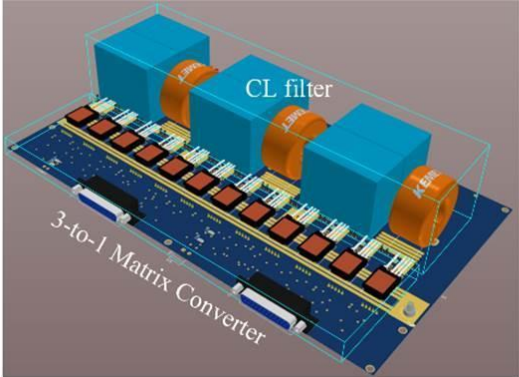
Studied Case	Electrical System Configuration	Performance of AC and DC currents																				
<p>Case 1: Centralized Single Converter</p>	 <p style="text-align: center;">Simulation Parameters for Four Cases</p> <table border="1" data-bbox="412 783 984 1251"> <tbody> <tr> <td>Grid voltage</td> <td>208V line-to-line</td> <td>AC Inductance</td> <td>0.3mH</td> </tr> <tr> <td>DC-link voltage</td> <td>55V</td> <td>AC Capacitance</td> <td>30uF</td> </tr> <tr> <td>Transformer turn ratio N:1</td> <td>2:1</td> <td>Leakage Inductance</td> <td>60uH</td> </tr> <tr> <td>Switching frequency</td> <td>20kHz</td> <td>AC Inductance</td> <td>5mH</td> </tr> <tr> <td>Rated Current</td> <td>50A</td> <td>AC Capacitance</td> <td>200uF</td> </tr> </tbody> </table>	Grid voltage	208V line-to-line	AC Inductance	0.3mH	DC-link voltage	55V	AC Capacitance	30uF	Transformer turn ratio N:1	2:1	Leakage Inductance	60uH	Switching frequency	20kHz	AC Inductance	5mH	Rated Current	50A	AC Capacitance	200uF	<p>Charging results:</p>  <p>Discharging results:</p> 
Grid voltage	208V line-to-line	AC Inductance	0.3mH																			
DC-link voltage	55V	AC Capacitance	30uF																			
Transformer turn ratio N:1	2:1	Leakage Inductance	60uH																			
Switching frequency	20kHz	AC Inductance	5mH																			
Rated Current	50A	AC Capacitance	200uF																			
<p>Case 2: AC-Parallel- DC-Parallel- Connected Converters</p>	 <p>* Power converter system uses two Iso-MCs and can handle double DC charging/discharging current. It also has improved AC current quality and low DC current ripples.</p>	<p>Charging results:</p> 																				
<p>Case 3: AC-Parallel- DC-Series- Connected Converters</p>	 <p>* Power converter system uses two Iso-MCs and can bear</p>	<p>Charging results:</p> 																				

	<p>double DC voltage. It also has improved AC current quality and low DC current ripples.</p>	
<p>Case 4: AC-Parallel-DC-Independent-Connected Converters</p>	 <p>* Power converter system uses two Iso-MCs and can have improved AC current quality. The DC current ripples are the same as in case 1.</p>	<p>Charging results:</p> 

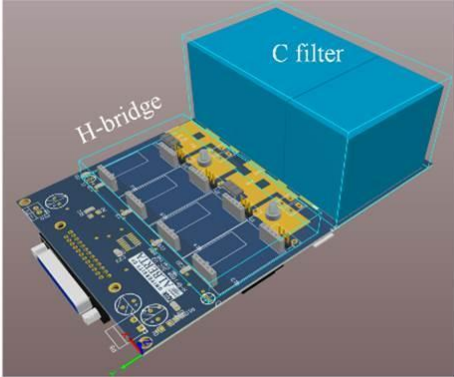
Future research plans: the first configuration is commonly adopted in reported works/projects (Nobuyuki Tokuda, 2002; Declan Bryans, 2018). On the other hand, the other three configurations also show some merits in terms of different stack layout. Therefore, in the future, they will be further investigated to find out the suitable configuration of the power converter for different types of VRFB stack configurations.

3.2.3 Hardware design

The hardware design of the main circuit of Iso-MC is divided into two parts: (a) 3-to-1 matrix converter part which contains the active switches and AC-side CL filters (see Fig.3.2.1.9(a)), (b) H-bridge converter part which contains the active switches and the DC-side C filters (see Fig.3.2.1.9(b)). The high-frequency transformer is selected with 400V:200V voltage ratio, 2.6μH leakage inductance, 4.6mH excitation inductance, and 20kHz operating frequency.



(a)



(b)

Fig.3.2.1.9. Hardware design of the main circuit of Iso-MC. (a) 3-to-1 matrix converter part, (b) H-bridge converter part.

The prototype of the 3-to-1 Matrix converter part is built in the lab (University of Alberta) for the scale-down verification and the hardware is demonstrated as in Fig.3.2.1.10.

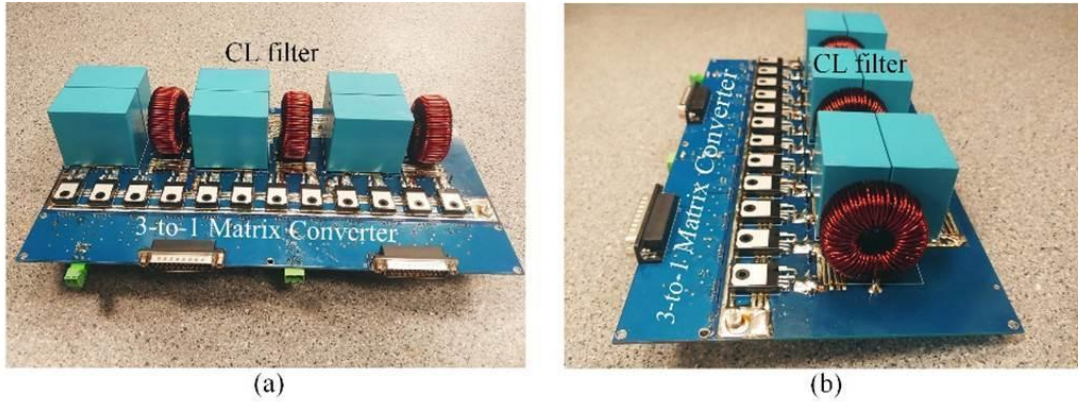


Fig.3.2.1.10. The prototype of the 3-to-1 Matrix converter part. (a) Front view, (b) side view.

3.3 Design of system controller considering cell voltage variation

3.3.2 Multi-loop control strategy for VRFB

To charge/discharge the VRFB, a constant current-constant voltage charging technique should be considered for the power converter (Md. Parvez Akter, 2019). This naturally divides the scheme into two control modes: one is constant-current-control mode, the other one is constant-voltage-control mode.

For the constant-current-control mode, the current reference should be provided based on the SOC of the battery as shown in Fig.3.3.2.1. While for the constant-voltage-control mode, the voltage reference should be given based on the SOC as demonstrated in Fig. 3.3.2.2.

However, the VRFB cell voltage has a large variation induced by SOC, which introduces disturbance to the control loop. To compensate for the variation, DC voltage feedback control can be adopted in the multi-loop control strategy as shown in the control diagrams in Fig.3.3.2.1 and 3.3.2.2. The DC voltage is sensed as variable and sent back to the voltage controller of both modes. Therefore, the disturbance can be offset.

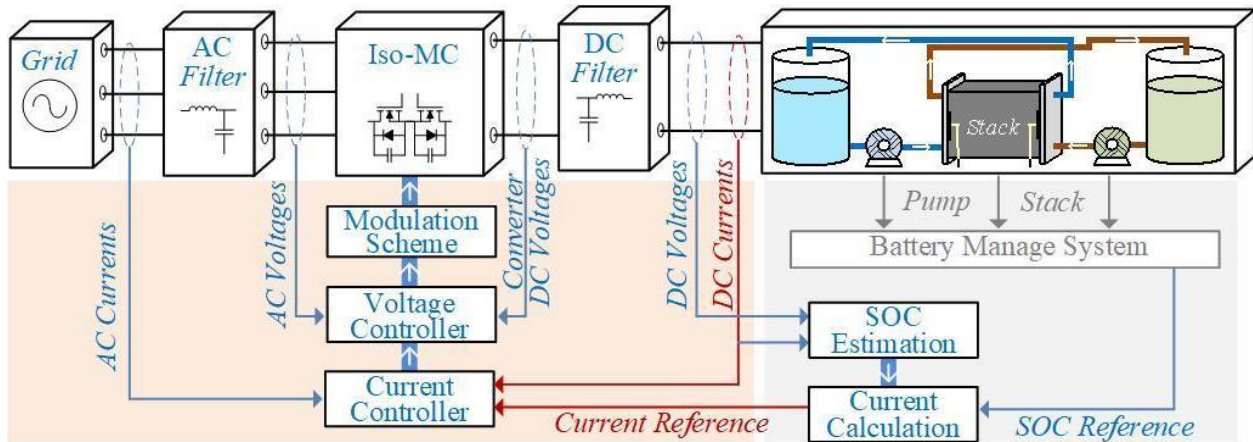


Fig.3.3.2.1. Constant-current-control mode of the multi-loop VRFB control strategy.

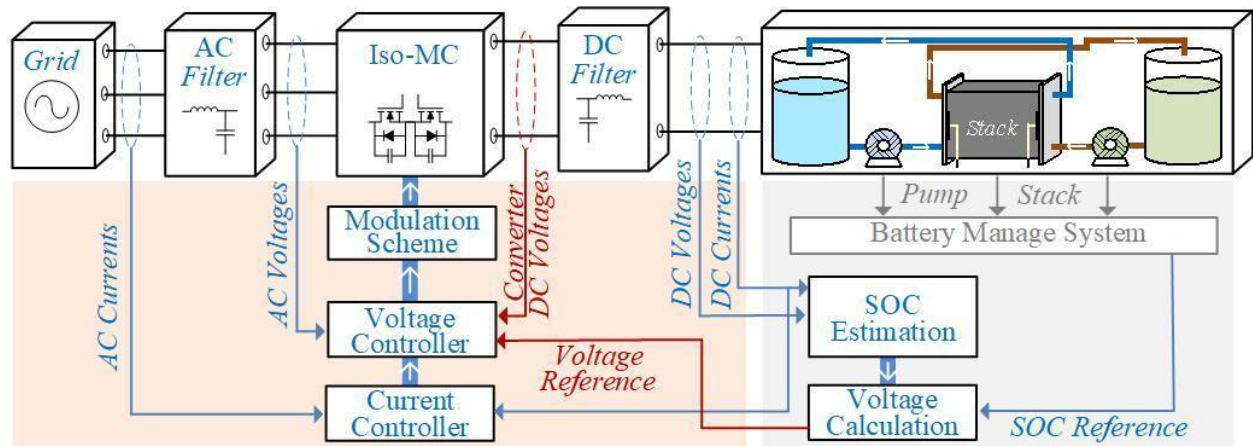


Fig.3.3.2.2. Constant-voltage-control mode of the multi-loop VRFB control strategy.

3.3.2 Optimal operation curve for VRFB

The performance of VRFB is related to many factors, e.g. temperature, flow rate, electrolyte concentration, etc. Among these, the operation current may potentially affect the power efficiency of the VRFB (Andrea Trovo, 2019). In another word, the current reference needs to be carefully chosen for charging/discharging control strategy, which will eventually lead to an optimal charging/discharging curve for VRFB.

To find out the suitable curve, the energy losses in VRFB should be thoroughly considered in terms of electrochemical reaction, mechanical equipment, power electronics. To be specific, the converter loss, pumping/piping loss, stack inner loss will be modeled and investigated in the VRFB system. The plan is to: (1) build the converter model in Power Analysis Software (e.g. PLECS), (2) include the electrical model of the VRFB stacks and pumping system, (3) utilize different charging/discharging curves to find out the tendency related to whole system efficiency, (4) conclude the optimal curve with reasonable values.

4. Use cases and Energy Management (EM)

4.1 Simulation tools

All scripts were coded with Python programming language and run in a computer Intel® Core™ i7 with 16 GB of RAM. The algorithms used to simulate the battery includes the recursive least squares (RLS), extended Kalman Filter (EKF), and Q-learning.

Simulation of the battery comprises two stages. Firstly, the battery is characterized and its internal electrochemistry modeled in order to determine its expected behavior in real applications. Secondly, battery's operational strategies are simulated considering real time demand and photovoltaic generation datasets.

Battery modeling. The main task of a battery management system (BMS) when controlling a battery energy storage system is providing accurate information about its state of charge (SOC), i.e., knowing what is the remaining amount of energy in the battery when discharging or the energy deficit when charging. SOC is a relative quantity defined as the remaining capacity over the nominal capacity of the battery and is usually measured in percentage.

SOC determination is a critical aspect to simulate battery applications and based on the fact that it relies on an accurate model, the Vanadium redox flow battery (VRFB) is being modeled by the electrical equivalent circuit model (ECM) in Fig. 4.1.1. The ECM is able to represent the static and dynamic characteristics of the battery with electrical components at a good trade-off between model's complexity and accuracy.

Static characteristics such as the battery open circuit voltage (OCV), ohmic resistance, and polarization resistance are represented by the ideal voltage source and R_o , respectively. The OCV depends on the battery SOC and temperature, R_o describes the internal battery resistance, i.e., is the resistance associated to the membrane, electrodes and contact between components. Dynamic characteristics are represented by the polarization resistance and capacitor network, R_p and C_p respectively, which represent the transient dynamics caused by the electrochemical processes that take place within the cell. The first-order model in Fig. 4.1.1 (n -RC, where $n=1$) is simplified to a Thevenin model for its analysis.

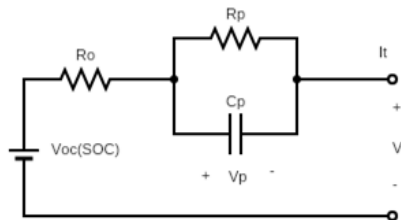


Fig. 4.1.1. Schematic diagram of the electrical ECM.

Based on the current and voltage Kirchhoff laws the model electrical behavior is described.

$$C_p \frac{dV_p}{dt} = I_t - \frac{V_p}{R_p} V_{oc} = R_o I_t + V_p + V_t$$

By solving and discretizing the solution is possible to determine the model parameters R_o , R_p and C_p , i.e., to characterize the system.

$$R_o = \frac{b_1}{a_1} ; R_p = \frac{a_1 b_0 + b_1}{a_1^2 + a_1} ; C_p = \frac{-a_1^2 T}{a_1 b_0 + b_1}$$

Model parameters are affected by temperature, current, flow rate, SOC and battery aging [1], therefore, in order to keep the model prediction accuracy such parameters are calculated on a real time basis with the recursive least squares (RLS) algorithm.

Battery OCV is a static characteristic broadly used to estimate the stack SOC since it describes the nonlinear relationship between the battery terminal voltage and the SOC at equilibrium state, i.e., when no current is flowing through the battery (nor charging neither discharging) for a period of time called standing time [2]. Such a relationship was obtained experimentally. The first experimental curve was partially obtained with 30-min standing time, however, due to time constraints and no significant changes the full experimental curve was obtained with 10-min standing time. From the same experimental curve, the RLS initial parameters R_o , R_p and C_p were extracted.

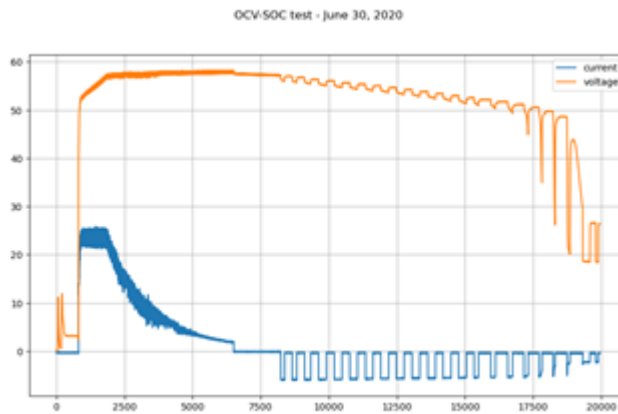


Fig. 4.1.2. 10-min standing time OCV-SOC curve

This method is extensively used for Lithium-ion batteries where standing time has been reported as 1-hour. Given the difference of electrolyte aggregation state for VRFB the 10-min may be enough.

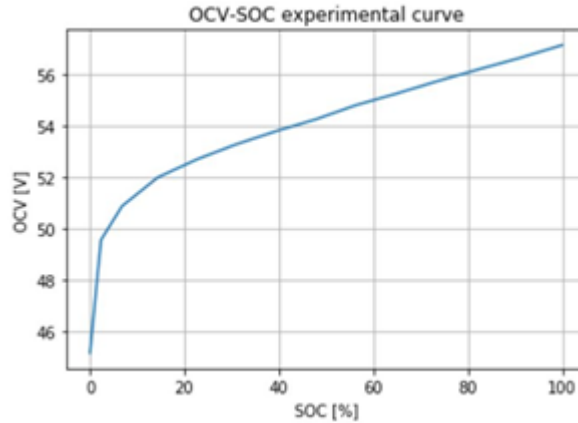


Fig. 4.1.3. Experimental OCV-SOC stack curve

Polynomial regression is the more extensively used method to determine SOC [3]. A third order grade polynomial was used because a higher order did not return higher accuracy, such coefficients are described in the following table.

$$V_{oc} = \sum_{i=0}^{n_p} c_i z^i ; \quad c_i \text{ is the polynomial coefficient; } n_p \text{ is the model order}$$

Constant	4.75393318e+01
Linear	3.30549991e-01
Quadratic	-5.12092573e-03
Cubic	2.81889199e-05

Table 4.1.1. Coefficients of the third order polynomial regression

There are several methods to estimate the battery SOC; the coulomb counting is a simple and extensively used method where the discharged current of a battery is measured and integrated over time. The main drawback of this method is the accuracy over time because it does not consider factors such as the battery cycle life.

$$SOC(t) = SOC(t - 1) + \frac{I(t)}{Q_n} \Delta t ; \quad Q_n \text{ is the capacity of the battery; } \Delta t \text{ is the time interval}$$

In this case, the instantaneous SOC is obtained with the coulomb counting method combined with the extended Kalman filter (EKF) algorithm according to the measured terminal voltage and current. EKF is a robust, accurate and broadly employed method in state estimation problems; it is an extension to the Kalman filter for nonlinear systems that handles random noise from the variation of battery model parameters and measurements.

In the state-space model for EKF, stack terminal voltage is the nonlinear system measurement denoted as y_k and the stack current is the system input \mathbf{u}_k . \mathbf{x}_k is the state vector, \mathbf{w}_k is the process noise, and v_k is the measurement noise. Process and measurement noise are zero-mean white Gaussian stochastic processes with covariance matrices Q_k and R_k . \mathbf{A} is the system matrix, \mathbf{B} is the control matrix, \mathbf{C} is the output matrix, and \mathbf{D} is the feedforward matrix.

$$\begin{aligned}
 \mathbf{x}_k &= F(\mathbf{x}_{k-1}, \mathbf{u}_{k-1}) \approx \mathbf{A}_{k-1}\mathbf{x}_{k-1} + \mathbf{B}_{k-1}\mathbf{u}_{k-1} + \mathbf{w}_{k-1} && \text{State equation} \\
 y_k &= G(\mathbf{x}_k, \mathbf{u}_k) \approx \mathbf{C}_k\mathbf{x}_k + \mathbf{D}_k\mathbf{u}_k + v_k && \text{Observation equation} \\
 \mathbf{w}_k &\sim (0, \Sigma_w) \\
 v_k &\sim (0, \Sigma_v)
 \end{aligned}$$

EKF implementation is based in the repeated evaluation of a set of equations: 1) estimation of the prior state, 2) estimation of error covariance matrix, 3) update Kalman filter gain, 4) estimation of posterior state, 5) update error covariance matrix.

Based on the one charge/discharge cycle measurements between 10 and 80% SOC, the estimated SOC, battery terminal voltage and power stack are shown.

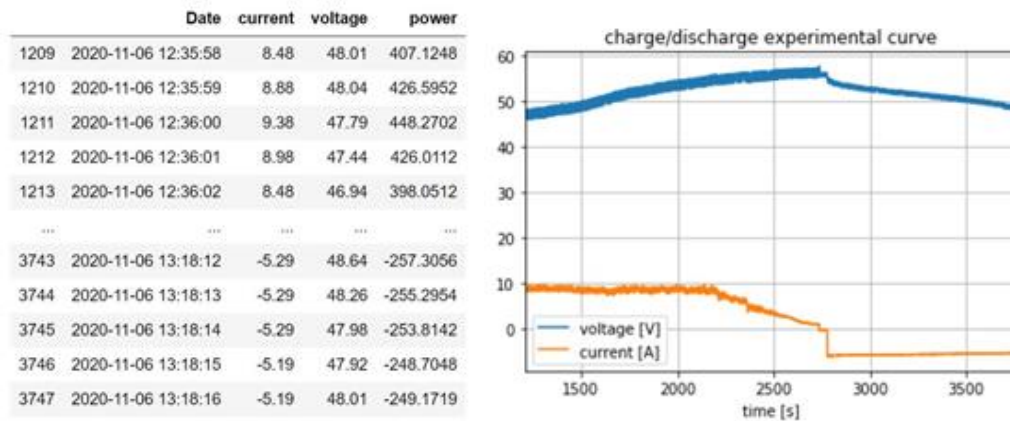


Fig. 4.1.4. Charge/discharge cycle, voltage and current measurements

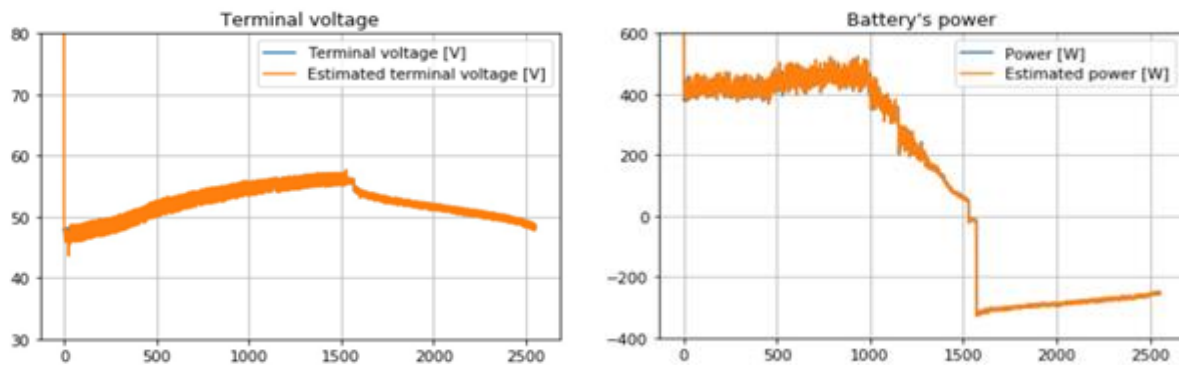


Fig. 4.1.5. Estimated stack terminal voltage and power

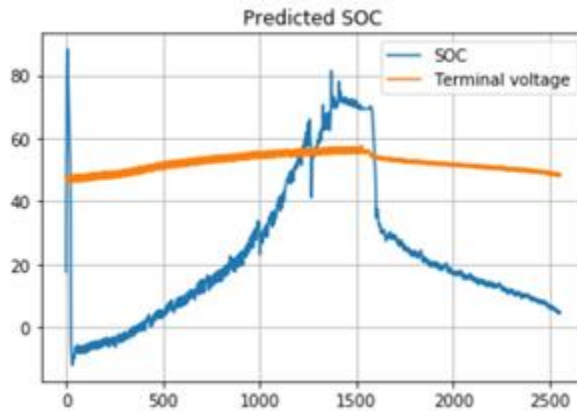


Fig 4.1.6. Predicted SOC

One of the weaknesses of the EKF method is the lack of tuning procedures, therefore Q_k , R_k and P_0 (initial error covariance matrix) were tuned based on trial and error.

4.2 Development of use cases and operation strategies

A total of 67 projects utilizing VRF battery technology were identified and classified in the survey based on their applications as shown in Fig. 1.2.1.

Depending on the author slightly different definitions of these use cases or applications were found, particularly between load shifting and peak shaving. Both applications, from the perspective of the final user can be applied to decrease the electricity monthly bill. However, peak shaving reduces the power consumption, whilst load shifting decreases the energy consumption during a given period of time to increase it when the cost of electricity is lower. In the second case there is no decrease of electricity consumption.

Regarding renewables integration, VRFB have been used mainly to smooth wind power integration into the grid [4] given its large discharge duration and the high number of life cycles. As the main drawback of this technology is its power and energy density, despite its lower cost of energy per cycle. Based on its advantages, VRFB technology is a good alternative for applications in the order of hundreds of kW where space to install the system is not a concern.

Suitable applications for VRFB are those requiring long-discharge durations and lower power densities, i.e., load shifting, renewables integration and power reliability such as UPS systems, battery backup and emergency power. Nonetheless, the shorter duration peak shaving application has been performed with this technology in some projects according to the survey.

Integration of distributed energy resources (DER) has been the main trend regarding electricity generation and consumption in several countries around the world by at least the last decade. Particularly in Alberta distributed generation based on solar technologies contributed 67.8 MW installed capacity in 2020 [5]. Regarding electricity consumption, residential energy demand was

the second largest sector in Canada after the industrial sector in 2018 [6], which is a trend that does not seem to change over time.

Despite this trend, the integration of solar distributed generation represents technical challenges in terms of stability for the power grid. Integration of battery energy storage systems is one of the highly researched solutions at the cost of augmented operational complexity.

According to Sun [7], load shifting is one of the most effective methods to manage peak demand, yet here is applied to the residential sector given its large potential contribution to the integration of DERs. Load shifting is strongly linked to the electricity rate structure, i.e., the battery operation strategy is based on the electricity price differences along a period of 24 hours. The potential benefits are two sided. On the one hand takes advantage of electricity price differences which implies that customers are able to reduce their electricity monthly bill. On the other hand, utility companies may increase the utilization factor of their assets, thus delaying infrastructure upgrade costs.

DERs integration in this case is discussed at the light of a grid-connected solar microgrid. The microgrid comprises a local residential consumer, a solar photovoltaic system and a Vanadium redox flow battery; all elements have the same operation objective and, it is assumed, are operated under a centralized controller. The objective is to maximize the monetary savings a residential consumer can obtain when electricity purchase from the grid is minimized at times when electricity tariff is higher and selling back any electricity surplus. This implies maximizing the use of PV electricity generated in-situ and storing any surplus of energy in the VRF battery for later usage, i.e., the battery is used to perform load shifting application. In this case, the microgrid is working on grid-tied mode looking for load balancing throughout a day.

The reference rate structure utilized in this research work for the electricity purchase from the grid is the time of use (TOU). Rates are separated in three bands:

- Off-peak from 7:00 pm to 7:00 am of the following day in summer and winter
- Mid-peak from 7:00 am to 11:00 am and 5:00 pm to 7 pm in summer, and from 11 am to 5 pm in winter
- On-peak from 11:00 am to 5:00 pm in Summer, and from 7:00 am to 11:00 am and 5:00 pm to 7 pm in winter

Summer season goes from May to October and winter from November to April. The difference between off-peak and mid-peak rate is around three cents/kWh and between off-peak and on-peak is circa seven cents/kWh [8].

The electricity sell strategy is driven by the feed in tariff (microFIT) program for solar rooftop projects less than 6 kW with a contract of 20 years [9]. Both tariff schemes are implemented in Ontario.

The proposed operational strategy implies that preference is given to the PV generation, which means the household first consumes the power delivered by the solar panel. In case there is a surplus of electricity and the battery SOC is low, the battery is charged. But if the PV power

generation is not enough to supply the demand and the battery energy content is sufficient then the battery backs the PV system at supplying the demand. Up to now, the battery has been charged at no cost or discharged to supply the demand considering that any resulting energy surplus from the load balance can be sold back to the grid at the FIT electricity price. The last scenario implies supplying the residential load and/or charging the battery with energy from the grid when the electricity rate is lower according to the TOU scheme before described.

The operational strategy is benchmarked with a grid-connected solar microgrid containing just a PV generation system and a residential load. The main performance metric to determine how effective this approach can be is comparing the profits made by the battery-agent system at performing load shifting versus the microgrid system with no agent, i.e., just balancing load with the PV system and the grid.

4.3 Simulation and evaluation of use cases and strategies

The proposed intelligent battery control problem has been formalized as a Markov decision process (MDP), which is a condition to guarantee convergence of the implemented reinforcement learning (RL) algorithm. A Markovian environment assumes the next state is completely determined by just the current state and current action, i.e., it has no influence from past state or actions.

MDP problem is reduced to finding an optimal policy $\pi(s)$ that gives back an action $a \in A$ for each state $s \in S$. A policy is the rule that defines the agent's behavior at a given time, in other words the policy maps states of the environment to actions the agent can take. Particularly the optimal policy corresponds to the expected return for the best action the agent is able to take in a state. One approach to find the optimal policy is given by solving the Bellman optimality equation, which is also the solution to the RL problem:

$$V(s) = \max_{a \in A} (R(s, a) + \gamma E[V(s') | s])$$

$s' = T(s, a, p')$ is derived from the transition function T , which defines the action the agent takes to transition from one state to another. However, neither the transition function is known nor is possible to compute the expectation in the equation. Therefore, one approach is solving the equation by means of the Q-learning algorithm.

Q-learning algorithm is considered a model-free algorithm where the agent has no previous knowledge of the environment, thus the agent is forced to learn from its experience based on the direct interaction with the environment. The selection of actions follows an ϵ -greedy policy with possible ϵ values between 0 and 1. Depending on the value of ϵ the agent performs more exploration (closer value to 1) or more exploitation (closer value to 0) in the environment.

In general terms, the agent observes the environment at time t , takes one possible action based on the ϵ -greedy policy and observes both, the next state and the reward $R(s, a)$, and tries to approximate the optimal action-value function Q^* by updating the corresponding q-value ($Q(s, a)$) to each state-action pair based on the equation:

$$Q(s, a) \leftarrow Q(s, a) + \alpha [R + \gamma \max_a Q(s', a) - Q(s, a)]$$

α is the learning rate that determines the weight of reward values over previous q-values. The design of the reward function is a critical component when working with the Q-learning approach. A reward is the value the agent receives from the environment when an action is taken, so it contains all the necessary information to conduct the decision-making process of the agent.

The action-state space is finite and discrete in this problem. The state space is a tuple containing five elements including the electricity generated in-situ by the PV system and the residential demand being balanced for the next minute, the electricity tariffs of TOU and FIT, and the battery SOC at time t .

$$s_t = [pv_t, demand_t, TOU_t, FIT_t, SOC_t]$$

The action space consists of the two possible actions the agent can take, charge or discharge. Battery charge and discharge rates were calculated from experimental data considering the battery capacity and the time it takes to fully charge and fully discharge at a constant current. At each time t the agent selects an action based on the ϵ -greedy policy, if the action implies the battery being outside of the battery's energy limits then the energy to charge or discharge is limited to the battery maximum and minimum capacity. In this part of the process the SOC is updated with respect to the charge or discharge rate.

Battery agent task is to schedule charge and discharge to back up the PV array at meeting the residential demand at all time; any electricity surplus can be exported to the grid and its monetary value is calculated with the FIT rate. Load is balanced with power from the grid in case the battery and the PV system are not able to meet the load; given this scenario, the deficit of energy should be imported to the microgrid and the related cost calculated with the TOU electricity tariff.

The microgrid with no battery behaves the same, any excess electricity is exported to the grid and the value associated is calculated with the FIT rate, whilst any deficit is imported from the grid and the associated cost is calculated with the TOU tariff.

The reward function accounts at each time step for the difference between the cost of imported and exported electricity by the agent in both microgrid systems. When the energy cost throughout the day is lower with the microgrid-battery system, the agent obtains a reward of 1, when the cost

is lower with the microgrid-PV system, the reward is -1. At the end of the day the rewards obtained at each time step are summed. Therefore, the agent is positively compensated every time it obtains cost savings with the battery system.

Load shifting is performed during the Summer and the Winter season based on one-minute resolution data to have the possibility of comparing the battery performance under different conditions and different pattern load profiles.

The demand profile and PV generation data correspond to a household located in Edmonton. Figures below presents the load profile and PV generation of one day in Winter (January 2018) with a demand of 23.67 kWh, and one day in Summer (August 2017) with a demand of 33.69 kWh.

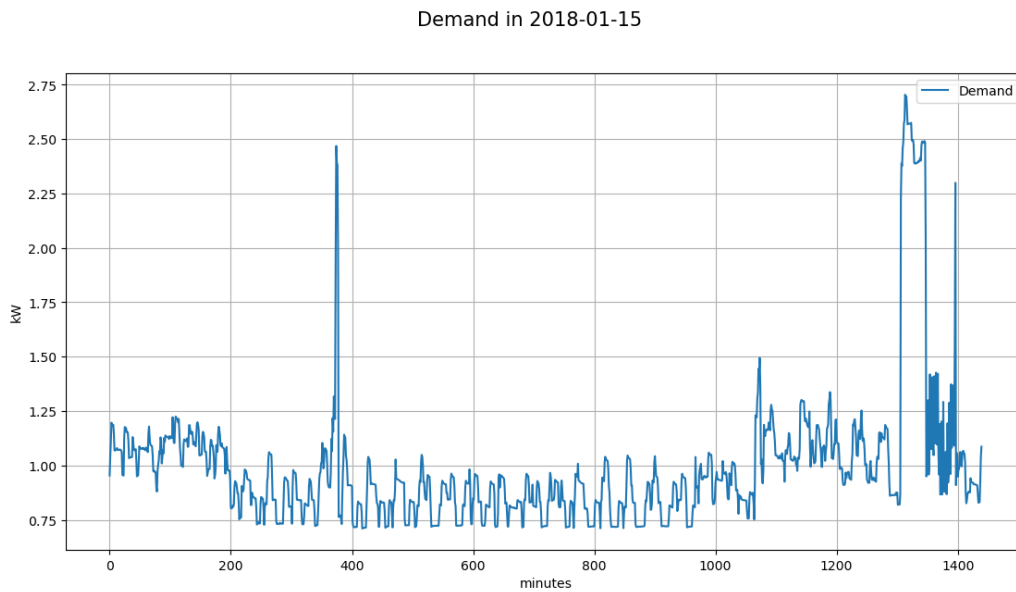


Fig 4.3.1. Residential load profile, January 2018

PV generation in 2018-01-15

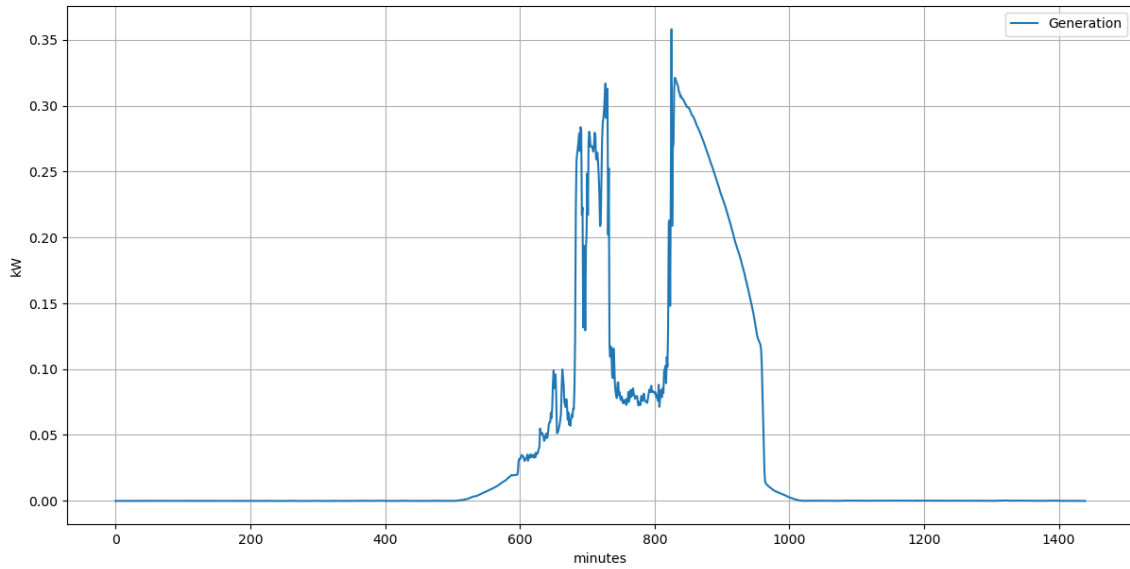


Fig 4.3.2. Photovoltaic generation profile, January 2018

PV generation in 2017-08-07

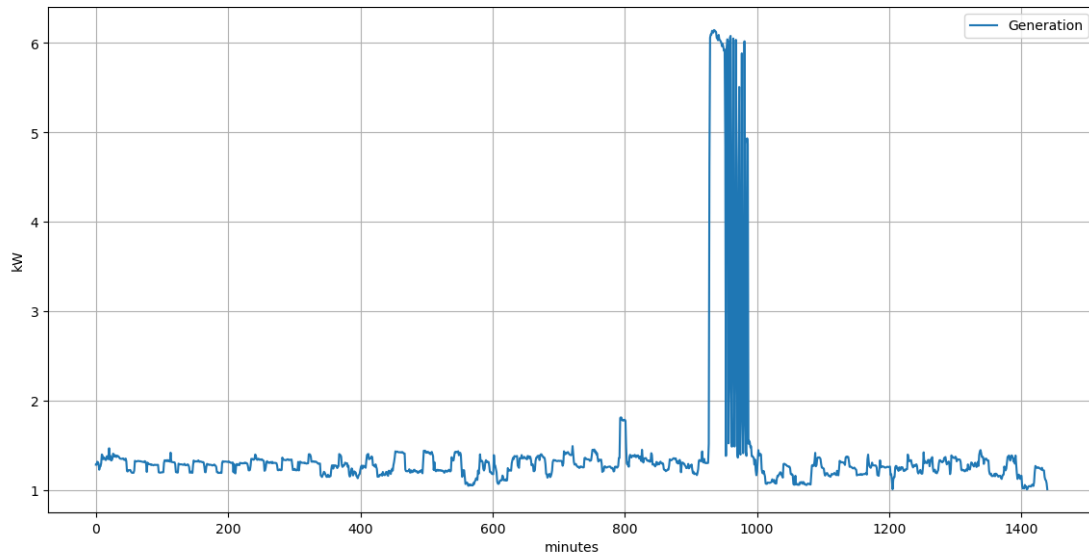


Fig 4.3.3. Residential load profile, August 2017

PV generation in 2017-08-07

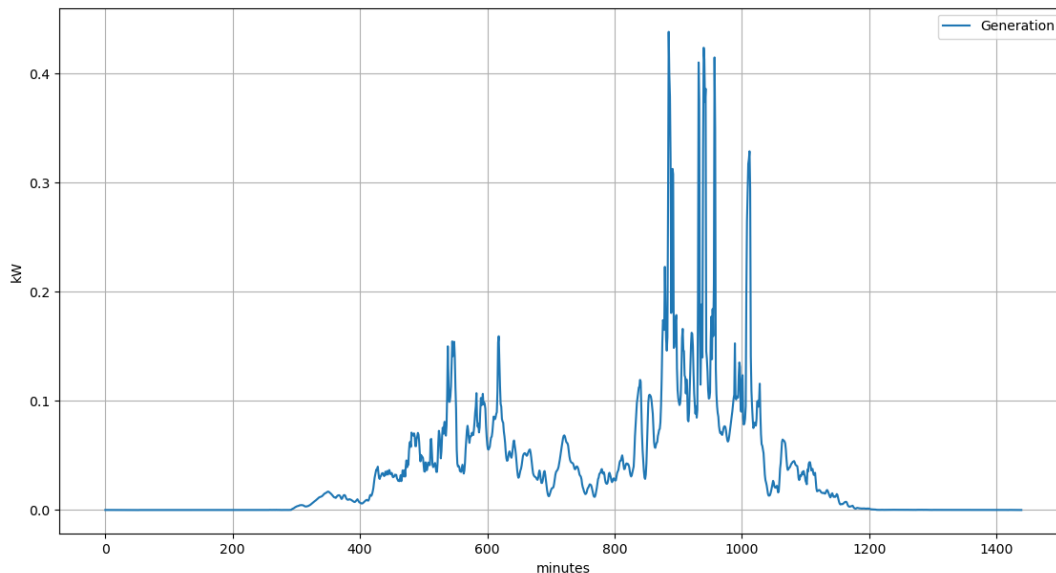


Fig 4.3.4. Photovoltaic generation profile, August 2017

The nominal power output of the stack is constant at 2.5 kW with a volume capacity of 86 L of electrolyte. This corresponds to an estimated capacity of 3.44 kWh and a discharge time of 85 minutes under nominal output power settings (50 A). Yet, the charge and discharge data were obtained with the battery using a fraction of its maximum nominal capacity, i.e., 40 L of electrolyte, maximum peak power of 775 W, discharge capacity of 475 Wh and battery efficiency of 82%. Discharge currents were varied between 6, 15 and a maximum of 47 A. Some simulations were performed with a higher battery capacity (49 kWh) in order to identify the feasibility of having a larger battery covering the electricity consumption.

Training demonstrates that the agent was able to find the optimal policy where the residential user can decrease its electricity costs during a day by charging the battery at times when electricity price is lower and discharging when the price is higher. This can be seen in the graphs below because the rewards obtained increased consistently over 10 000 episodes and during the repetition of the simulations to get consistent results. In the long run the minimum and maximum rewards tend to the mean.

Regarding the tested battery capacities, the higher battery capacity obtained higher rewards because savings are higher than those obtained with the lower battery capacity. This is possible as long as one of the technical characteristics of VRFB is that capacity can be increased just by pouring more electrolyte in the reservoirs.

Between Summer and Winter season it can be seen that during Winter the reward is slightly higher than in Summer. This behavior can be explained by the higher consumption in the Summer

day, particularly during a few hours during the evening, which implies a more efficient energy management with the battery during the Winter day.

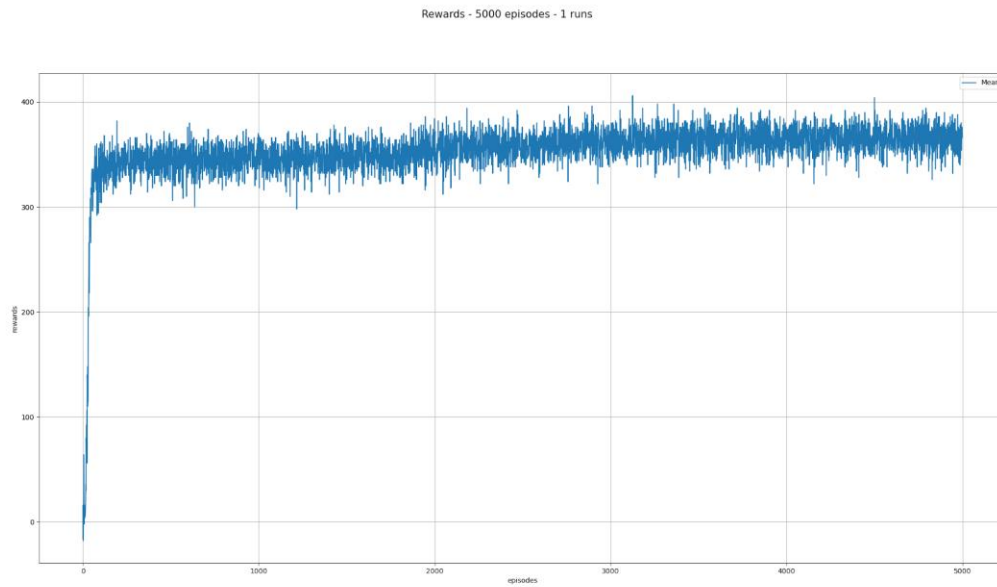


Fig 4.3.5. Rewards with lower battery capacity, experimental capacity in Winter season

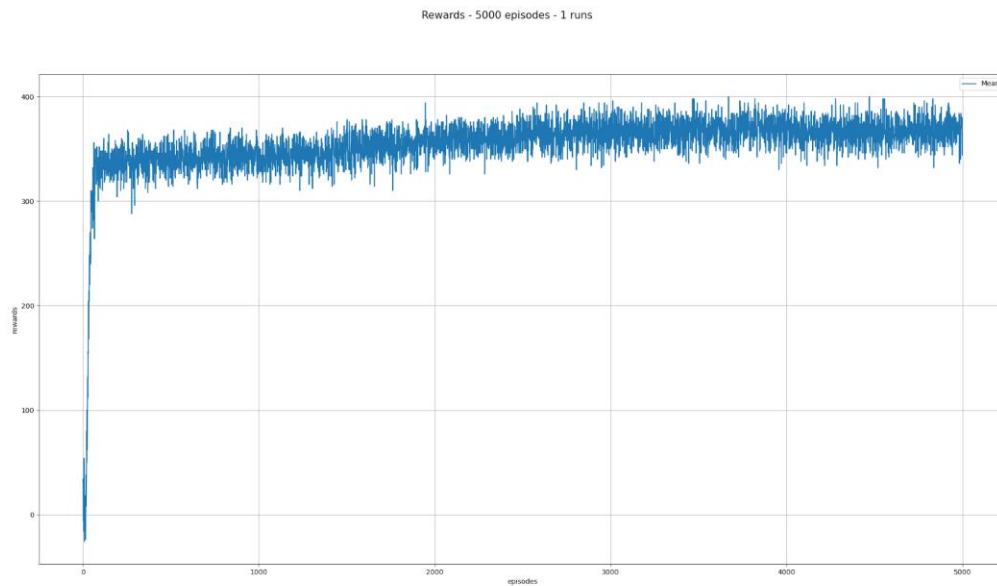


Fig 4.3.6. Rewards with higher battery capacity in Winter season

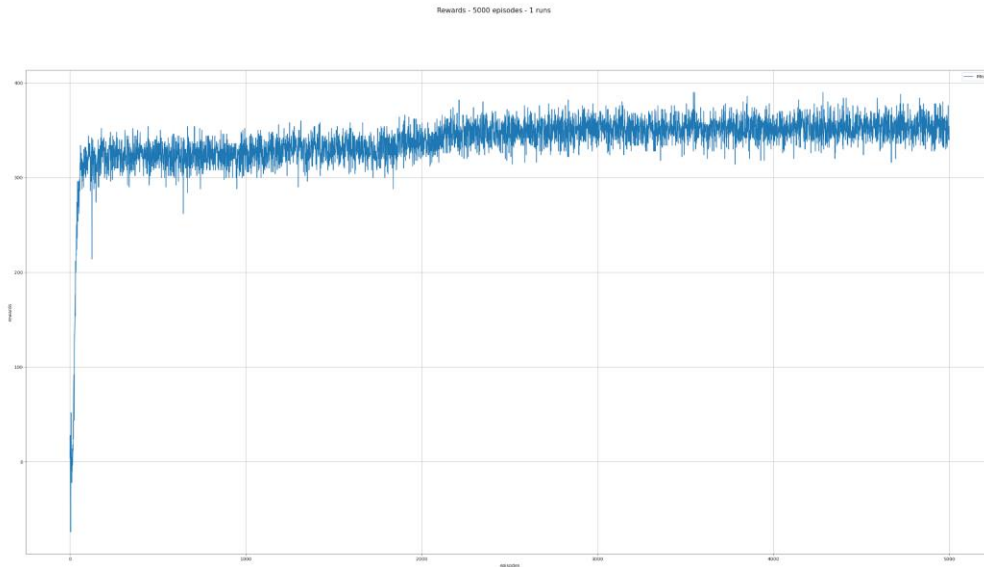


Fig 4.3.7. Rewards with higher battery capacity in Summer season

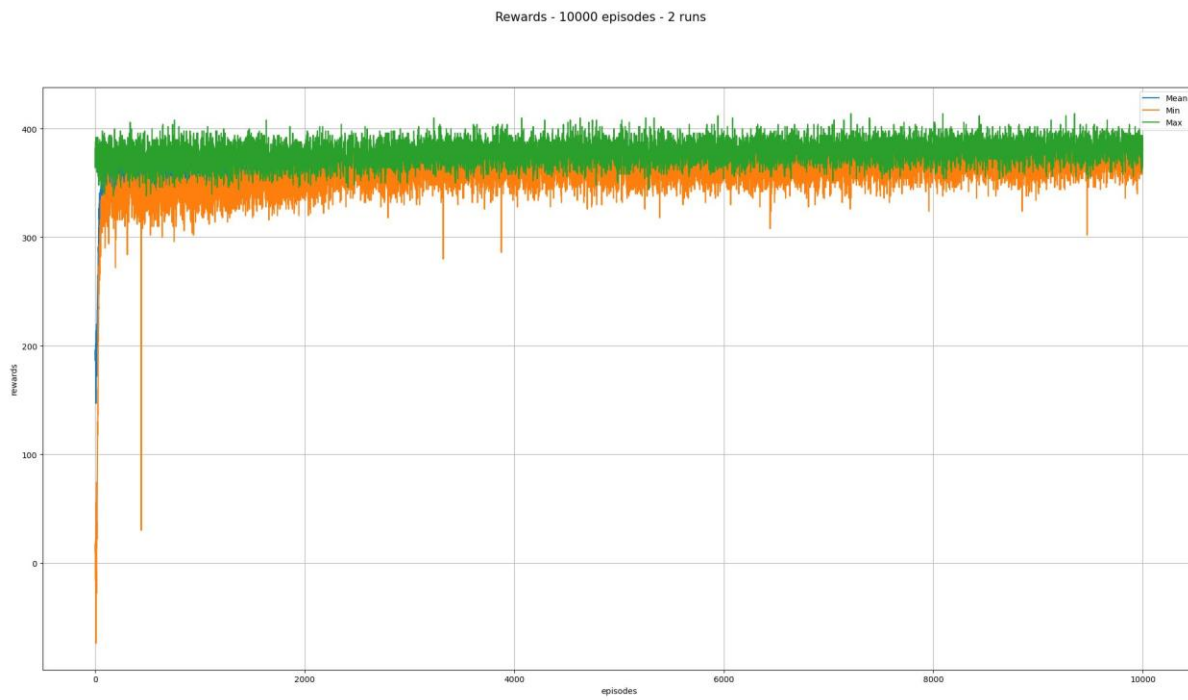


Fig 4.3.8. Rewards obtained by the agent - a day in Winter season

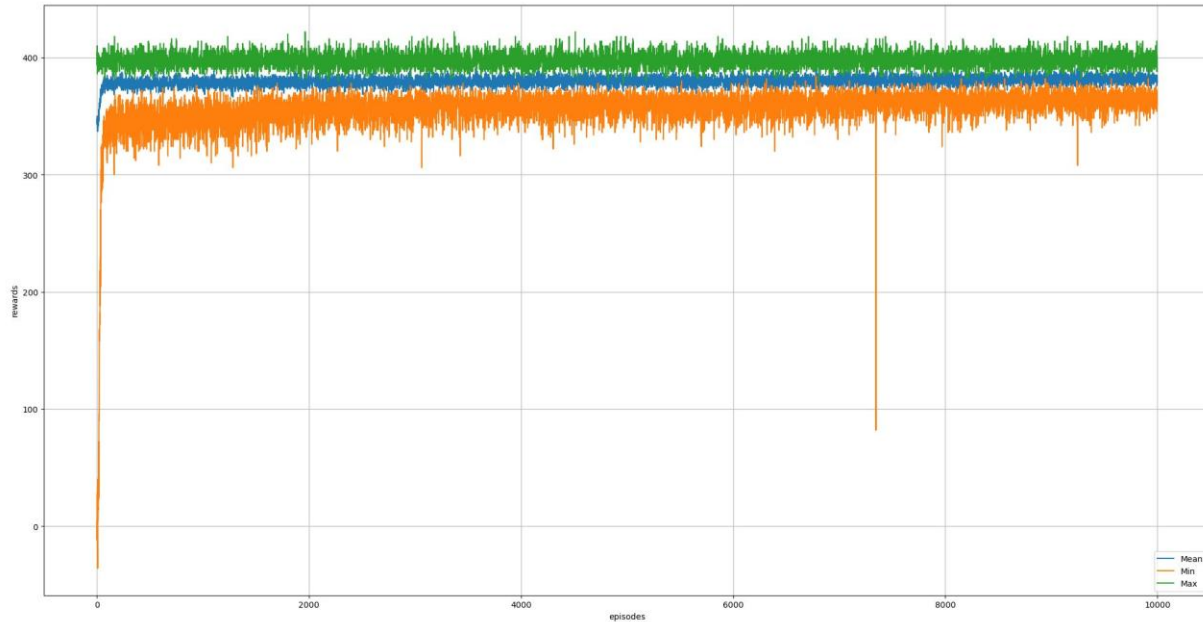


Fig 4.3.9. Rewards obtained by the agent - a day in Winter season

4.4 Stakeholder engagement, dissemination

Progress and results of this project have been presented to the public and professional communities in the province at a number of occasions:

SPARK 2019: Under the title “Flexible batteries to power the renewable transition” and as part of the Future Energy Systems at the University of Alberta, the Vanadium redox flow battery (VRFB) project participated in the SPARK conference hosted in Edmonton at the end of October 2019. The conference, organized by the Emissions Reduction Alberta (ERA), featured a number of energy transition topics and clean technology innovation in general. VRFB showcase pursued to inform the audience about the technical features and potential environment benefits of the technology toward decarbonizing the power sector.



Photo by Kenneth Tam

Telus WoS: In Summer 2019, the VRFB project showcased at the TELUS World of Science Edmonton that hosted a short course called Research Zone in partnership with the UAlberta Energy Week. During the Research Zone training eighteen graduate students and post-doctoral fellows acquire skills that let them to communicate with public audiences, mainly children and youth. The presentation of the VRFB project to kids provided full explanations about how their homes are electrified and the possibilities to store electricity for future use.

APIC: Members of Alberta Power Industry Consortium (APIC) are the major electric power utilities in the province. They include Alberta Electric System Operator (AESO), AltaLink, ATCO Electric, Enmax, EPCOR, and FortisAlberta. Information on this project has been provided to the member companies at a number of venues through the project duration.

5. Additional Topics

5.1. SOC Sensing - Motivation & Techniques

The VRFB employs a single-metal system with two soluble redox states, reducing the cross-contamination issues found in hybrid systems while maintaining superior stability and reversibility. Furthermore, solid state reactions are eliminated and the electrodes are not prone to damage during deep-discharge in contrast to intercalation-type materials used in other battery technologies. However, the high voltages present during overcharging may promote side reactions such as oxygen/hydrogen evolution, decreasing the electrolyte lifetime.

One of the most common and simple techniques for avoiding overcharge is to track and limit the voltage during the charging process. The voltage is chemistry dependent and can be modelled via the Nernst equation (equation 5.1) at zero current. While the stack voltage during cycling is dependent on the current, the open-circuit voltage (OCV) can be monitored with a separate single-cell operating at zero current.

$$E = E^0 + \frac{RT}{nF} \ln\left(\frac{[V^{5+}][H^+]^2[V^{2+}]}{[V^{4+}][V^{3+}]}\right) \quad (5.1)$$

When the system is balanced (each tank has identical amounts of electrochemically available vanadium ions), the state of charge can be expressed as equation 5.2. This allows a relationship to be formed between the OCV and state of charge (SOC) via modification of the Nernst equation (equation 5.3). However, this method produces inaccuracies due to incomplete representation of the electrode potential, and is only accurate when the system is balanced (equation 5.2).

$$SOC = \frac{[V^{2+}]}{[V^{2+}]+[V^{3+}]} = \frac{[V^{5+}]}{[V^{4+}]+[V^{5+}]} \quad (5.2)$$

$$E = E^0 + \frac{RT}{nF} \ln\left(\frac{SOC^2([H^+]+SOC)^2}{(1-SOC)^2}\right) \quad (5.3)$$

Capacity losses due to imbalanced ion/water transfer through the membrane are easily mitigated via periodic remixing of the electrolytes, or via a hydraulic shunt between the electrolyte tanks (Figure 2.4.4b). However, some capacity-loss mechanisms are asymmetrical (disproportionately affects one electrolyte tank), such as: V^{2+} oxidation via atmospheric oxygen (negative electrolyte), V^{3+} reduction via hydrogen evolved at negative electrode, V^{5+} precipitation as V_2O_5 in the positive electrolyte. In order to maintain the indefinite lifetime of the electrolyte, these mechanisms must be mitigated with chemical or electrochemical methods. However, domination of a particular mechanism causes the equality of equation 5.2 to break down, and the OCV will no longer accurately depict the SOC. Furthermore, it is not possible to detect these imbalances via OCV. To detect the onset of these imbalances, an ideal system should be capable of monitoring the SOC of each electrolyte individually.

Theoretically a reference cell could be placed into each tank, but would be impractical due to reference potential drift and poor sensitivity [11]. A four-pole device has been used to measure the voltage difference across the electrolyte (with inert inner poles) when a current is applied through the outer poles. Although eliminating the polarization effect and measuring the actual potential arising from the solution characteristics, this method has poor sensitivity due to low potential changes over the course of cycling and measurements are very sensitive to the current (lower currents have poor sensitivity while higher currents give inaccurate measurements). Potentiometric titration with potassium permanganate is a popular approach, but is intrusive, requires time, and is thus unsuitable for real-time continuous monitoring [12].

Since electrolyte composition and proton concentration vary over the course of cycling, conductivity could be monitored and correlated to SOC. However, probe calibration is required to make precise measurements [11,12]. The composition changes also result in color changes which can be observed with the naked eye (green → violet and blue → yellow for the positive and negative electrolytes respectively). Absorbance of the solutions can be monitored and correlated to the SOC. If one has access to a spectrometer to generate/analyze multiple wavelengths, monitoring of the negative electrolyte is very simple due to a linear relationship at 410 nm [13]. The positive electrolyte displays a parabolic relationship at 754 nm [13] and for wavelengths in the 300-850 nm range [11], and as such must be compared against voltage vs time data for SOC estimation.

In non-scientific cases where cost is a major factor, a white light source and photodiode detector could be used to simplify the design. This concept was developed and discussed in section 2.4.2. The main issue of this technique is the high absorbance of the electrolyte. Because of this, absorbance measurements must be done through a thin cross section of the electrolyte (ex <1 cm [13]) to ensure accurate data acquisition.

5.2: SOC (Light) Sensor

5.2.1: Sensor design

A flow-through type cell was created in order to visualize the electrolyte (Figure 5.2.1a). A U-shaped reservoir was constructed by hollowing 6"x6" silicone gaskets (variable thickness configurations). Endplates were constructed with 6"x 6"x $\frac{1}{2}$ " clear acrylic sheets. The hollow gaskets (and $\frac{1}{16}$ " acrylic support sheet in thick configurations) are sandwiched between the endplates with $\frac{1}{4}$ " diameter bolts, and $\frac{1}{2}$ " tube inlet/outlets are machined into one plate to allow for electrolyte flow.

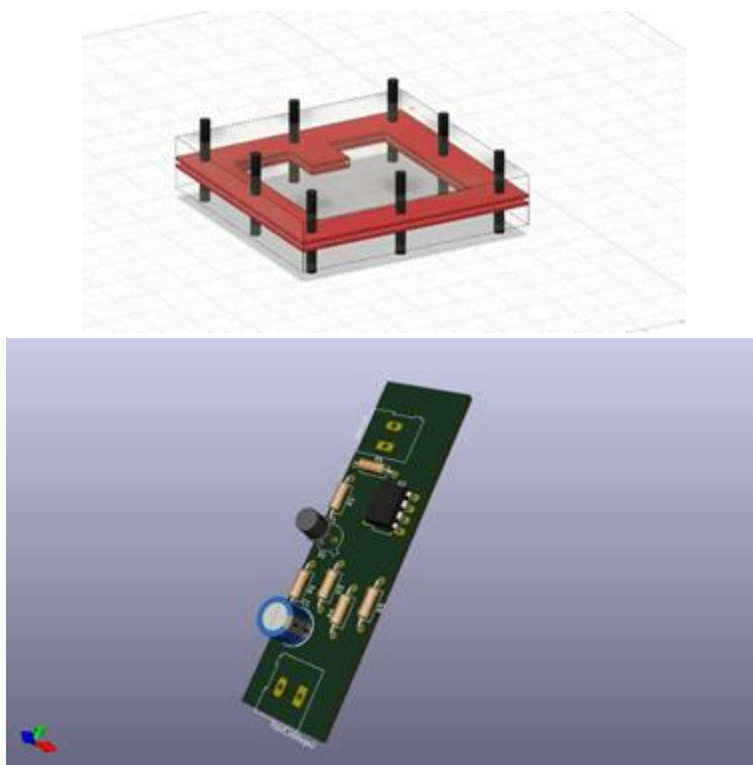


Figure 5.2.1: a) SOC light sensor flow cell configuration; b) Detector PCB layout

A white LED light source can be shone through one side of the flow cell, and the transmitted light can be detected via a photodiode on the other side of the cell. A photodiode PCB was constructed (Figure 5.2.1b). A noise filter was created with a 1k Ω resistor and 0.1 μ F capacitor and placed under a 24 V reverse bias voltage. An operational amplifier was later added to improve the obtained results.

5.2.2. Experiments and Results

At low and high SOC values, the positive electrolyte becomes very bright and has high light transmittance. At moderate SOCs, V(IV)/V(V) complexing causes the electrolyte to become very dark and little/no data can be obtained in this region for a 1/4" flow thickness and no amplification (Figure 5.2.2a). The negative electrolyte displays much lower absorbance changes, but data can be obtained for a wider range of SOC values. In order to improve the results, the flow thickness can be reduced. This results in larger sensitivity and more data coverage (Figure 5.2.2b). This test also illustrates the need for proper alignment of the light source/detector, as any changes may result in a voltage offset between experiments. Future testing should include the development of a housing that ensures consistent detector/light source placement.

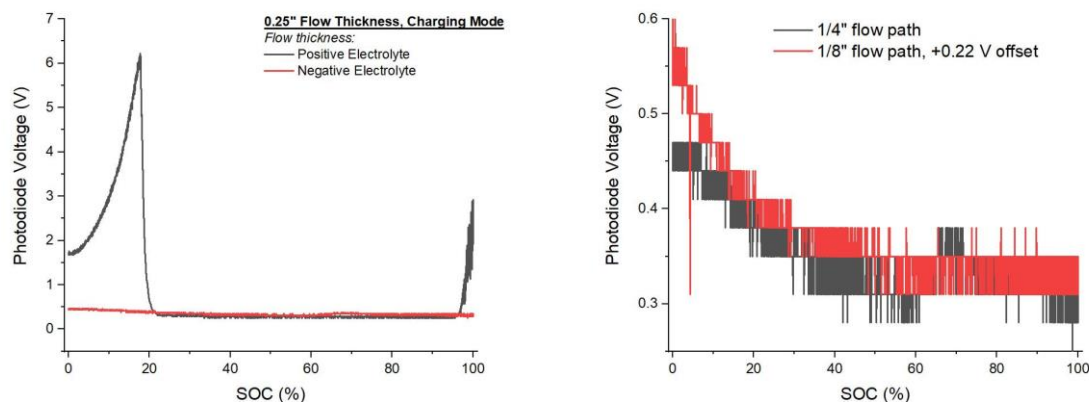


Figure 5.2.2: SOC light sensor results. a) comparison of positive and negative electrolytes with 1/2" thickness; b) comparison of negative electrolyte with 1/4" and 1/8" thicknesses

These experiments did not make use of an operational amplifier, which should increase the data sensitivity. Future experiments should also make use of smaller flow thicknesses. Optical paths of 0.5 cm and 1 cm (0.2-0.4") are the most commonly used in literature, and flow thicknesses in this regime should result in full or near-full data coverage. One downside of reducing the thickness is the simultaneous reduction of flow rate, which must be considered to avoid the requirement of a secondary pump.

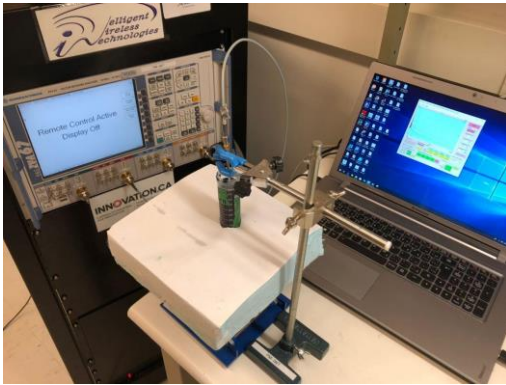
5.3. Microwave SOC Sensor

5.3.1: Design and Analysis

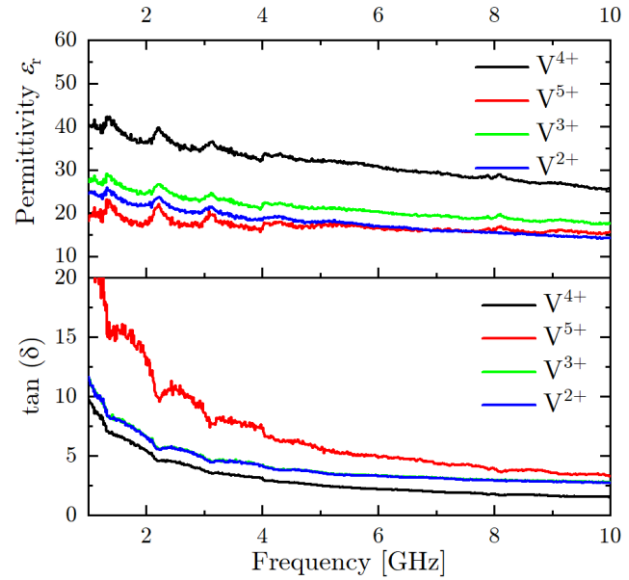
A complementary split ring resonator (CSRR) is designed as the main sensing element of the reflective sensor. CSRRs are metamaterial inspired particles that enable highly sensitive regions with respect to dielectric variation.

The choice of frequency for CSRR is tied to the dielectric properties of the MUT that decreases with frequency. Thus, a relatively high value of 6 GHz is opted considering fabrication tolerances of small size features.

Dielectric probe measurements are conducted to measure the loss factor of each material in the tanks, including charged (V^{5+}) and discharged (V^{4+}) solutions in the *positive* tank as well as charged (V^{3+}) and discharged (V^{2+}) solutions in the *negative* tank. Separation between the two extreme states inside the positive tanks, namely V^{5+} and V^{4+} is much higher than that of the other tank, thus effective sensor response is expected to be more pronounced using samples in this tank. Based on the dielectric properties of these solutions measured with dielectric probe at 6 GHz, charged solution V^{5+} is characterized with $\epsilon_r = 17 - j85$, while discharged solution V^{4+} measured $\epsilon_r = 30 - j66$. Even though their permittivity is considerably different, yet the magnitude of loss in either state of Vanadium redox process is high enough to overshadow the permittivity that prohibits regular mode of operation in the sensor to distinguish them. Therefore, there is a need to overcome this concern in microwave frequency, which brings us to the negative resistance design in the sensor to enhance its performance.



(a)



(b)

Fig. 5.3.1 (a) Dielectric probe setup, (b) Dielectric property measurement

In order to increase the sensitivity of the sensor to lossy medium, the dissipated power in the sensor is compensated with a negative resistance circuit using ATF34143 as shown in Fig. 5.3.2. Loss compensation in the CSRR can be viewed as the level of restoring the lost power in the resonator at the frequency of resonance that is directly modifying the depth of reflection. Therefore, the main goal of this study is to decrease the depth of S11 notch, where small capacitive/resistive variations brought about by the MUT are considerably distinguishable.

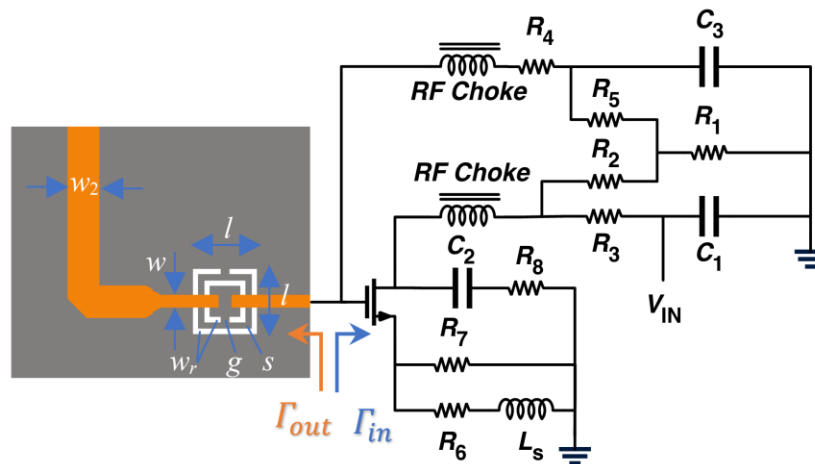
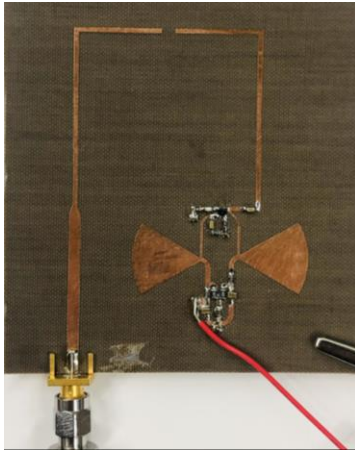
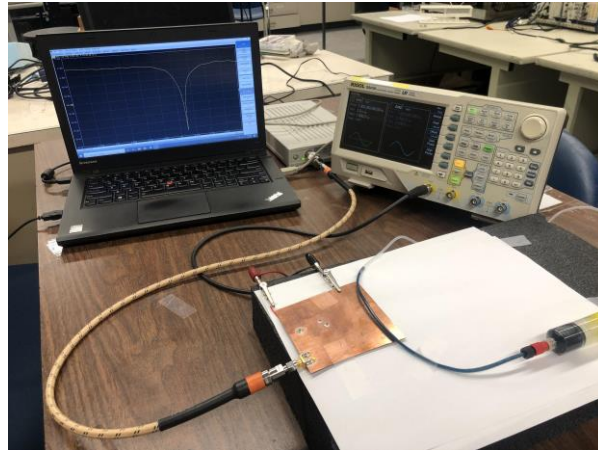


Fig. 5.3.2. Schematic of the active sensor



(a)



(b)

Fig. 5.3.3. (a) Fabricated Sensor top, (b) Measurement Setup

5.3.2. Results and Discussion

The proposed sensor is fabricated on Rogers 5880 with dielectric properties of $\epsilon_r = 2.2$, $\tan(\delta) = 0.0009$, and 0.8 mm thickness. It is noteworthy that all transmission lines as well as the circuit elements are on the top side of the substrate, while the CSRR is etched out of the ground plane on the other side (see Fig. 5.3.3).

The vanadium redox liquids are exposed to the sensor using PTFE tubing fixed at the top of the substrate and OD = 1.6 mm and ID = 0.8 mm. Two extreme cases in vanadium redox liquids include positively charged and discharged solutions. Based on the dielectric properties of these solutions measured with dielectric probe at 6 GHz, charged solution V^{5+} is characterized with $\epsilon_r = 17 - j85$, while discharged solution V^{4+} measured $\epsilon_r = 30 - j66$. Even though their permittivity is considerably different, yet the magnitude of loss in either state of Vanadium redox process is high enough to overshadow the permittivity that prohibits regular mode of operation in the sensor to distinguish them. Therefore, negative resistance is activated to enhance the sensor dynamic range. Fig. 5.3.4 showcases the difference in S_{11} profile for the two liquids, which is in agreement with their dielectric loss tangent. Charged solution holds more charges and becomes more lossy (with $\tan(\delta) \sim 5$) while the discharged state is at lower loss level (with $\tan(\delta) \sim 2.2$). This is captured with the sensor where higher loss in MUT is shown with lower depth of S_{11} .

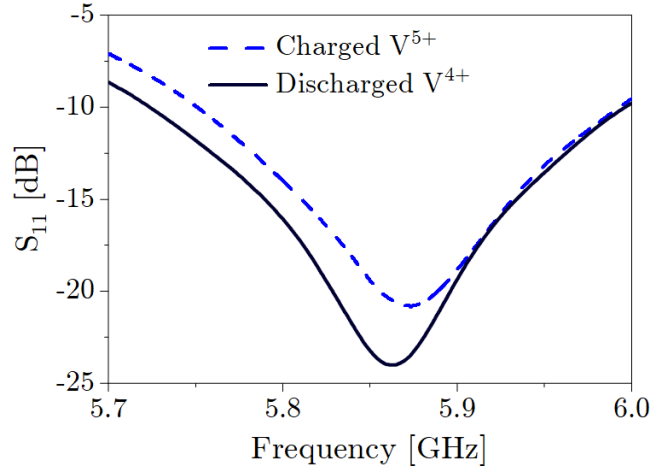


Fig. 5.3.4. Measurement Results

5.4: Alternative Current sensor

5.4.1: Sensor Design

During the operation and testing of the optical SOC sensor, the Voltarion stack controller board was damaged and rendered inoperable. DC voltage coming out of the stack was still readable by the Texas instruments ADC as it was able to withstand the charge and discharge voltages. The DC current measurement was not able to be directly measured by the TI ADC. Since the current produced would be DC and is connected through a single wire circuit to the charging/discharging circuit, current measurement through induction was possible by the use of a Helmscoil. This coil was placed around one of the leads and produces a voltage that can be safely measured but the ADC.

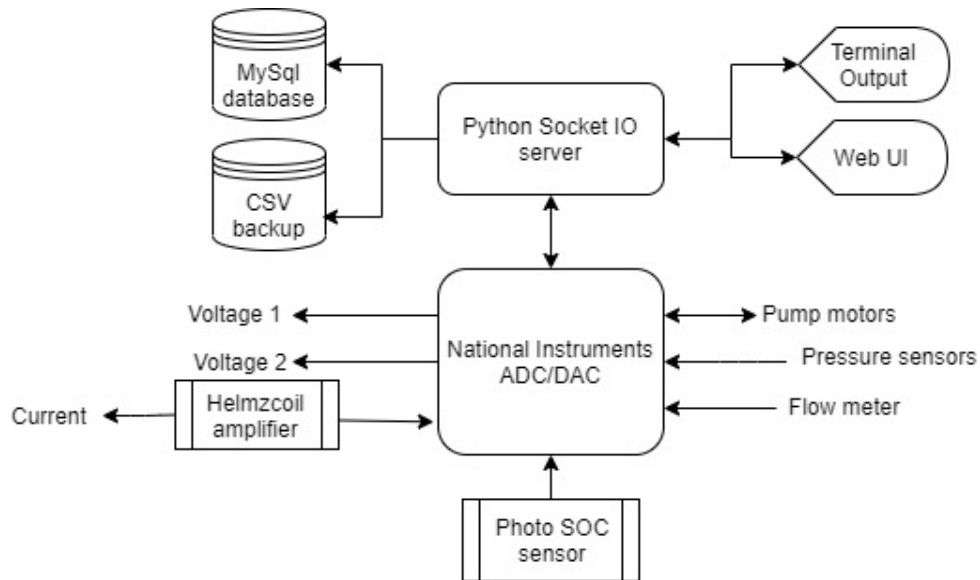


Figure 5.4.1: System changes after Voltarion control board failure.

The voltage that was produced by the coil was found to be too narrow of a range to be able to capture the operating region of the charging and discharging current. An amplification circuit was designed and built to be able to record the full current range with the Texas Instruments ADC. The system was tested and was ready to be deployed, however COVID 19 restrictions and subsequent inability to access the system installed on the test site prevented the installation of the sensor.

6. Conclusions

This project was designed to address knowledge gaps associated with Vanadium for Redox Flow Batteries (VRFB) as electric storage devices in comparison with other electricity storage approaches.

The conducted survey of found that VRFB brings a number of advantages, especially in stationary applications with long expected lifecycle. In addition to cycling and cost considerations, VRFB technology also excels in terms of safety and environmental impact at the end of its life. In addition to the study of research literature, a technology and market survey was also executed to complement the review.

The VRFB system has been assembled on an industrial test site and operated to gain experience and to conduct experiments aimed to characterize the installed system and to develop and test use cases and strategies. A number of experiments have been performed to examine performance of the battery system during charging and discharging. The system was connected to the mains using a commercial power converter acquired for the project. In addition, research was conducted to design new inverter topologies that take into account specific properties and characteristics of VRFB systems to increase its power rating, and to improve efficiency and improve cell balancing. In parallel with the experiments, simulation models of the VRFB system have been developed for design and modelling of use cases and operation strategies of the system.

In addition to the activities directly addressing project objectives, additional tasks have been included to deal with issues encountered during project execution. The first was design of an alternative current sensor necessitated by damage to the original control board. The second was development of a state-of-charge sensor that would be necessary for an effective integration of VRFB system in many different applications.

The results of the project were disseminated through a number of stakeholder communities, including research literature, electric utilities, and general public.

7. References

- [1] Z. B. A. Z. C. M. S. L. T. M. & S.-K. M. Wei, " Real-time monitoring of capacity loss for vanadium redox flow battery.," *Journal of Power Sources*, pp. 390, 261-269., 2018.
- [2] R. & S. W. Xiong, *Advanced battery management technologies for electric vehicles.*, John Wiley & Sons., 2019.
- [3] R. X. B. L. B. C. L. L. Y. Z. W. .. & W. M. Zhang, "A study on the open circuit voltage and state of charge characterization of high capacity lithium-ion battery under different temperature.," *Energies*, vol. 9, no. 2408, p. 11 , 2018.
- [4] L. J. & M. P. E. Ontiveros, "Modeling of a vanadium redox flow battery for power system dynamic studies.," *International journal of hydrogen energy*, vol. 39, no. 16, pp. 8720-8727, 2014.
- [5] C. E. R. I. (CERI), "Opportunities and challenges for distributed electricity generation in Canada," <https://ceri.ca/assets/files/Study%20187%20Full%20Report.pdf>, 2020.
- [6] C. E. Regulator, <https://www.cer-rec.gc.ca/en/data-analysis/canada-energy-future/2020/results/index.html>.
- [7] Y. W. S. X. F. & G. D. Sun, "Peak load shifting control using different cold thermal energy storage facilities in commercial buildings: A review.," *Energy conversion and management*, vol. 71, pp. 101-114., 2013.
- [8] O. E. Board, <https://www.oeb.ca/rates-and-your-bill/electricity-rates>.
- [9] IESO, <https://www.ieso.ca/en/Get-Involved/microfit/Program-Documents>.
- [10] Bhattarai, A., Ghimire, P., Whitehead, A., Schweiss, R., Scherer, G., Wai, N., & Hng, H. (2018). Novel approaches for solving the capacity fade problem during operation of a vanadium redox flow battery. *Batteries*, 4(4), 48. doi:10.3390/batteries4040048
- [11] Skyllas-Kazacos, M., Kazacos, M. (2011). State of charge monitoring methods for vanadium redox flow battery control. *Journal of Power Sources*, 196(20), 8822-8827. doi:10.1016/j.jpowsour.2011.06.080
- [12] Ngamsai, K., & Arpornwichanop, A. (2015). Measuring the state of charge of the electrolyte solution in a vanadium redox flow battery using a Four-pole cell device. *Journal of Power Sources*, 298, 150-157. doi:10.1016/j.jpowsour.2015.08.026
- [13] Shin, K., Jin, C., So, J., Park, S., Kim, D., & Yeon, S. (2020). Real-time monitoring of the state of charge (SOC) in VANADIUM REDOX-FLOW batteries using Uv–vis spectroscopy in OPERANDO MODE. *Journal of Energy Storage*, 27, 101066. doi:10.1016/j.est.2019.101066